12-17-2021 9:30 AM

Behaviour of Transmission Line Conductors under Tornadoes

Dingyu Yao, *The University of Western Ontario*

Supervisor: El Damatty, Ashraf A., *The University of Western Ontario*

A thesis submitted in partial fulfillment of the requirements for the Master of Engineering Science degree in Civil and Environmental Engineering

Abstract

Transmission line (TL) structure failures caused by tornadoes have been observed in multiple countries around the globe. The objective of this study is to develop an accurate load case that can simulate the critical tornado forces transmitted from the TL conductors to the towers. In order to achieve the goal, three different tornado wind fields, which were previously developed using computational fluid dynamic simulations, are considered. The tornado wind field provides the most critical forces on the TL conductors is determined and considered to obtain the critical load cases. Using the critical wind field, parametric studies are conducted to identify the tornado position that generates peak longitudinal forces. A parametric study is conducted on two different transmission line systems to assess the influence of conductor parameters on the longitudinal forces. Results of the parametric study are used to develop charts, which together with a three-dimensional interpolation procedure can estimate the critical conductor longitudinal forces on the towers.

Keywords: Transmission line, conductor, longitudinal forces, tornado, critical tornado load cases.

Summary for Lay Audience

Tornadoes are rapidly rotating columns of air extending vertically from the surface to the base of a cumuliform cloud. Transmission Lines (TLs) play an important role in transmitting electricity from the source of power to the distributing system. In current days, the reliance of the society on electricity is vital and extended interruption of electricity can cause devastating economic losses and social consequences. Due to the length of TL structures that extends for kilometers, there is a large chance that one of the TL towers gets exposed to the tornado. A large number of TL failures caused by tornadoes have been reported in Canada and worldwide. Triggered by the past failure events, an extensive research program was conducted at the University of Western Ontario to study the behaviour of TLs under tornadoes. The provision for critical tornado load cases that was introduced recently in the American Society of Civil Engineering design guidelines for TL was one of the achievements of this research program. As part of this program, the objective of the current study is to refine these new provisions pertaining to tornadoes by providing accurate means for estimating the loads transferred from the conductors to a TL tower during tornadoes. In order to achieve that, parametric studies are first conducted to analyze the response of TL conductors under different tornadoes. The tornado wind field and its corresponding position that provides the most critical longitudinal forces on the TL conductors are determined. Using these critical tornado configurations, the influence of conductor parameters on the longitudinal forces is then studied. Finally, the results of the parametric study are used to develop a simple and yet accurate approach to calculate the peak conductor longitudinal forces on the towers.

Co-Authorship Statement

This thesis has been prepared in accordance with the regulations for an Integrated Article format thesis stipulated by the School of Graduate and Postdoctoral Studies at Western University. Statements of the co-authorship of individual chapters are as follows:

Chapter 2: Response of transmission line conductors under different tornadoes

The CFD simulation tornado wind fields were proposed by Dr. H. Hangan, Dr. JD. Kim, Dr. A. Hamada, Dr. A.A. El Damatty, Dr. AY. Shehata and Dr. N. Ezami. The numerical model of conductors was proposed by Dr. H. Aboshosha and Dr. A.A. El Damatty. Drafts of Chapter 2 were written by D. Yao, and modified by Dr. A.A. El Damatty.

Chapter 3: Longitudinal reaction on conductors due to tornado wind load

The numerical model of conductors was proposed by Dr. H. Aboshosha and Dr. A.A. El Damatty. The analysis was conducted by D. Yao under the supervision of Dr. A. A. El Damatty. Drafts of Chapter 3 were written by D. Yao, and modified by Dr. A.A. El Damatty.

Acknowledgement

I would like to express my deep gratitude to my research supervisor, Dr. Ashraf El Damatty, for his advice and guidance throughout the past years. During the research work I have learned a lot from him, and his encouragement had helped keep me going when I struggled with my research.

The help and valuable advice I received from Dr. Nima Ezami are also acknowledged with sincere gratitude. I owe him a lot for his support and technical knowledge. It was a great pleasure working with him.

The support of my parents is deeply appreciated. Without their support I could not accomplish my research.

List of Tables

List of Figures

List of Symbols and Abbreviations

HIW	High Intensity Wind
TL	Transmission line
UWO	University of Western Ontario
CFD	Computational Fluid Dynamics
DOW	Doppler on Wheels
RANS	Reynolds Averaged Navier-Stokes
STV1	Stockton, KS 2005 tornado
GCV1	Goshen County, WY 2009 tornado
FEA	Finite element analysis
Vt	Tangential velocity of tornado
Vr	Radial velocity of tornado
Va	Axial velocity of tornado
$V_{resultant,max}$	The maximum resultant velocity of tornado
$R_{tn,max}$	radius where the maximum tangential velocity occurs
s	Swirl ratio
ls	Length scale of tornado
vs	Velocity scale of tornado
R	Tornado distance relative to the tower of interest
R_{max}	The tornado distance corresponding to the peak vertical velocity profile acting on the tower
θ	Angle between tornado center relative to the tower of interest
β	Angle between tornado center relative to the conductor's nodal point

r	Radius of the cylindrical coordinate
z	Height of the cylindrical coordinate
H	Conductor height
E	Young's modulus
w	Conductor weight per unit length
d_p	Projected diameter of conductor
S	Sag ratio
L	Span length
h	Insulator length
R_x	Conductor's longitudinal reaction
R_y	Conductor's transverse reaction
H_{cr}	The conductor height corresponding to maximum reaction
R_{x1}	Cable longitudinal force under tornado critical configuration corresponding to specific design group (d_{pmin}, w_{min}, S_{min})
R_{x2}	Cable longitudinal force under tornado critical configuration corresponding to specific design group (d_{pmax}, w_{min}, S_{min})
R_{x3}	Cable longitudinal force under tornado critical configuration corresponding to specific design group (d_{pmin}, w_{max}, S_{min})
R_{x4}	Cable longitudinal force under tornado critical configuration corresponding to specific design group (d_{pmax}, w_{max}, S_{min})
R_{x5}	Cable longitudinal force under tornado critical configuration corresponding to specific design group (d_{pmin}, w_{min}, S_{max})
R_{x6}	Cable longitudinal force under tornado critical configuration corresponding to specific design group (d_{pmax}, w_{min}, S_{max})

R_{x7}	Cable longitudinal force under tornado critical configuration corresponding to specific design group (d_{pmin}, w_{max}, S_{max})
R_{x8}	Cable longitudinal force under tornado critical configuration corresponding to specific design group (d_{pmax}, w_{max}, S_{max})
$R_{x(1-2)}$	Cable Longitudinal reaction corresponding to the selected design group minimum weight per unit length, minimum sag ratio, and the line's actual projected diameter
$R_{x(3-4)}$	Cable Longitudinal reaction corresponding to the selected design group maximum weight per unit length, minimum sag ratio, and the line's actual projected diameter
$R_{x(5-6)}$	Cable Longitudinal reaction corresponding to the selected design group minimum weight per unit length, maximum sag ratio, and the line's actual projected diameter
$R_{x(7-8)}$	Cable Longitudinal reaction corresponding to the selected design group maximum weight per unit length, maximum sag ratio, and the line's actual projected diameter
$R_{x(Smin)}$	Cable Longitudinal reaction corresponding to the selected design group minimum sag ratio, the line's actual weight per unit length, and the line's actual projected diameter
$R_{x(Smax)}$	Cable Longitudinal reaction corresponding to the selected design group maximum sag ratio, the line's actual weight per unit length, and the line's actual projected diameter
$Rx,_{numerical}$	The longitudinal reaction obtained using numerical technique
$Rx,_{graphs}$	The longitudinal reaction obtained using graphs

Chapter 1

1 Introduction

1.1 Background

Transmission Lines (TLs) play an important role in transmitting electricity from the source of power to the distributing system. In current days, the reliance of the society on electricity is vital and extended interruption of electricity can cause devastating economic losses and social consequences. As shown in Fig 1-1, a transmission line systems consist of towers, conductors, ground wires and insulator strings. The typical towers in a TL system are called tangent towers. The conductor system between those towers is continuous. In TL segment, tangent towers are bound by two end towers, which serve to contain the failure that might progress along the tangent towers. As exposed structures, TLs are often subject to severe weather events include wind storms. During those storms strong wind loads act on both the towers and the conductors. The conductor loads will transfer to the tangent towers through the insulators. Among wind storms, High Intensity Wind (HIW) events represent a major hazard to TL structures. HIW events include downbursts and tornadoes. Downbursts are formed by a cold jet of downdraft air while tornadoes is formed by a hot updraft of twisting air. They both often happen during thunderstorms. Those HIW events are localized and they affect a relatively small area unlike large-scale events such as hurricanes. As such, the design of typical structures does not account for the load produced by those events as the probability for an isolated structure to get exposed to a HIW event is small. However, the situation with TL structures is different due to their length that extends for kilometers. During a HIW event, there is a large chance that one of the towers of the line gets exposed to the event. Since the towers are connected by conductors, the failure of one tower cane lead to a progression of failures for other towers in the line. Therefore, it is important to consider HIW loads in the design of TL structures. Only recently, some provisions for critical tornado and downburst load cases were introduced in the American Society of Civil Engineering, ASCE-74 (2020) guidelines for transmission line. Those provisions, which represent the first specifications in the world for HIW TL loads, resulted from the research conducted during the past fifteen years at the University of Western Ontario (UWO), by Dr. El Damatty and his research group. The main objective

of this Thesis is to refine the new ASCE-74 (2020) provisions pertaining to tornadoes. In particular, the Thesis focuses on providing accurate means for estimating the loads transferred from the conductors to a tower during tornadoes. A unique situation occurs regarding the conductor's behaviour, which does not exist in large-scale wind events. The tornado will create loads that are not equal and not uniform along the ahead and back spans of a tower. Due to that, the transverse wind loads acting on the conductors will create unequal tensile forces in the ahead and back spans, which will result in a net longitudinal force acting on the tower. Given the complexity of this problem, in terms of wind loading and structural behaviour, it is difficult for engineers designing TL towers to estimate this force. As such, the current Thesis focuses on this aspect pertaining to the design of TL structures under tornadoes. In this Chapter, a literature review related to the tornado wind fields, the structural analysis of TL conductors, and the response of TL structures to tornadoes is provided. This is followed by the objectives and the scope of the Thesis.

Figure 1-1 Transmission line system
https://en.wikipedia.org/wiki/Transmission_tower#/media/File:Transmission_tower.jpg

1.2 Literature review

1.2.1 Tornado wind field

A tornado is defined as a rapidly rotating column of air extending vertically from the surface to the base of a cumuliform cloud (American Meteorological Society, 2021). Such localized wind events possess characteristics of short-lived, narrow path and complicated velocity profiles. The tornado consists of three velocity components: tangential, radial, and axial (vertical) components. Due to the complexity of the profiles of those three components, the wind loads acting on a transmission line are highly affected by the position of the tornado center relative to the transmission line system.

The most widely used scale for tornadoes classification is the Fujita scale, which was proposed by Fujita (1981). He established tornado categories based on the wind speed and the produced damage. Depending on the wind speed and the observed damage, a specific tornado can be classified as F0-F5, where F0 represents light damage while F5 represents the most severe damage. As stated by Doswell et al. (2009), the Fujita scale has the limitation of ignoring the construction quality. When the tornado path does not overlap buildings and bring damage, it might be misclassified at a lower category. Minor et al. (1993) has shown that the damage of some tornado categories can be caused by a lower wind speed than the corresponding Fujita scale wind speed. Due to the limitation of the Fujita scale, the new Enhanced Fujita scale was first introduced in 2007 (Potter, 2007). Instead of fitting damage to predetermine the wind speed, the Enhanced Fujita scale estimates the wind speed based on the damage (McDonald et al., 2010). The EF scale's main advantage is that it provides a large number of damage indicators. However, the Enhanced Fujita scale has not been widely used in the guidelines yet. The velocity of each category of the Fujita scale is presented in Table 1-1. In the latest version of ASCE, it was mentioned that 86% of the tornadoes that happened in the United States are classified as F2 or smaller (ASCE, 2020). Hong et al. (2021) reported that 80% of the reported tornadoes in Canada possess a smaller intensity than F2. Therefore, the current Thesis focus on F2 tornadoes.

Table 1-1 Wind speed for each category of Fujita scale

Fujita Scale	3-s gust Wind Speed (km/h)
F0	64-116
F1	117-180
F2	181-253
F3	254-332
F4	333-418
F5	419-512

In Canada, there is a relatively high possibility of tornado occurrence. Newark (1984) studied tornadoes that occurred in Canada from 1950 – 1979, which provides the first sight of Canadian tornado distribution. The results indicated that F3 or higher tornadoes happen in Ontario every 3.3 years on average. Cao and Cai (2011) proposed an upward trend in Ontario tornado frequency after studying the tornado data of 1950-2007 in Ontario. Hong et al. (2021) studied the tornado events between 2010 to 2019, and concluded that there is a 42.8 annual tornado occurrence rate for Canada. Considering the high possibility of a tornado crossing a transmission line system, the risk of transmission line failure due to tornado wind load is inevitable (Twisdale, 1982).

The tornado in-site velocity data was hard to obtain due to the limitation of measurement equipment. As technology developed, Wurman et al. (1997) proposed a new mobile Doppler Radar system design to obtain reliable tornado wind field data. This new deployment of Doppler radar is capable of recording two-dimensional traveling vertical wind profiles. Later, the mobile multiple Doppler network and Doppler On Wheels were proposed (Wurman, 2001). The Doppler radar quickly became a commonly used method to evaluate the tornado velocity, which contributed to many in situ tornado wind field data (Wakimoto et al., 2011, Wurman and Alexander, 2005, Lee and Wurman, 2005). However, the data obtained from the measurements mainly focus on tornado genesis instead of the wind velocity, while the latter is vital for structure analysis.

Therefore, using numerical simulation to estimate detailed tornado wind velocities provides another good option. The computational fluid dynamic (CFD) technique is widely used in conducting tornado simulations. Lewellen (1997) first developed a two-dimensional symmetric numerical model for vortices simulation. In the following years, many other researchers proposed two-dimensional models for tornadoes (Rotunno, 1977, Leslie and Smith, 1982, Wilson and Rotunno, 1986). Later, three-dimensional simulations were developed (Grasso and Cotton, 1995, Sarkar et al., 2005, Xia, 2001). The development of doppler enables validating the numerical simulation with actual measurement. However, the relationship between an actual tornado and a tornado simulation remained unknown for a long time. Hangan and Kim (2008) first use the swirl ratio as a parameter to ensure the experimental tornadoes have the same structure and characteristics as field tornadoes. They developed a CFD model for the Spencer, South Dakota F4 tornado, where the detailed tornado field data was provided by Sarkar et al. (2005). By matching the length scales between the Doppler radar data and the simulation, Hangan and Kim (2008) estimated the swirl ratio and the length scale of the tornado model that best represents the actual tornado. The velocity scale is then determined by matching the maximum tangential velocity of the numerical model and the full-scale data. Later, Hamada et al. (2010) modified the CFD model and rescaled it into the F2 category, which is one of the tornado wind fields used in this study and is called the Design Tornado..

There are three simulated tornado wind fields considered in this Thesis. In addition to the Design Tornado, the other two are the Stockton tornado which occurred in Kansas, USA, 2005, and the Goshen County tornado which occurred in Wyoming, USA, 2009. The radar data for these two tornadoes are first analyzed by Refan et al. (2014). El Damatty et al. (2018) developed numerical CFD simulations of those two tornadoes and determined the corresponding swirl ratio, length scales and velocity scales following the same procedure introduced by Hangan and Kim (2008). Due to the complicated velocity profiles and vortex structures, different tornado wind fields can provide different conductor responses and consequently different forces transferred to the towers. The tornado configuration that leads to peak conductor forces also can vary. As such, it is necessary to consider multiple tornadoes and tornado positions to obtain the most critical tornado load cases.

1.2.2 Structural analysis of TL conductors

The structural analyses of TL conductors under HIW have been conducted by a number of researchers using different means. Shehata et al. (2005) used a two-dimensional consistent curved beam element, developed by Koziey and Mirza (1994) and then modified by Gerges and El Damatty (2002) to include large displacement behaviour, to model conductors under downbursts. Each conductor span was divided into ten consistent beam elements. The conductors were analyzed twice in two different directions separately: horizontal direction to estimate the response under radial velocities, and vertical direction to estimate the response under vertical velocities and own weight. The insulator strings were simulated using two perpendicular non-linear springs, which form a three-dimensional pendulum. Six spans were considered. Shehata et al. (2005) have shown that this number of spans is suitable to estimate the forces transmitted from the conductors to the tower. Decoupling the horizontal and the vertical analysis was suitable for downbursts since the radial velocities of downbursts are much higher than the vertical velocities. However, this two-dimensional model cannot be used in the analysis under tornado loads due to the significant vertical velocity component of tornadoes. Thus, three-dimensional nonlinear cable elements were then employed to model the TL conductors under tornadoes (Hamada et al., 2010). This three-dimensional model of conductors was developed using the finite element commercial program SAP2000 (CSI, 2016). The model accounts for the large displacement and the P-delta effects, as well as the pretension stiffness and sagging. In this model, the insulators are simulated using two-node three-dimensional truss elements. The connection between the insulators and the tower cross-arms is simulated using intermediate hinge, which allows rotation in two perpendicular planes. Each cable span was divided into thirty cable elements. However, such finite element analysis (FEA) is very time consuming because of the large parametric study required in a tornado analysis which involve moving the tornado location in space.

An effective semi-analytical technique is then proposed and validated by Aboshosha and El Damatty (2014). This technique considers a three-dimensional multi-spanned conductor system, where the insulators are modeled as rigid pendulums that can rotate freely. In this technique, the longitudinal force at the end of the conductor is evaluated by satisfying the

moment equilibrium of conductors and insulators. The resulting equations are nonlinear and coupled, thus an iterative technique is applied to solve them. This semi-analytical technique takes into account the nonlinear behavior as well as the large deformation of conductors. One of the main advantages of this technique is its high efficiency. It is 185 times faster than the previously mentioned FEA. Due to the localized nature of tornadoes, the relative position of tornado center to the tower of interest greatly affects the response of the conductors. As such, the analysis needs to be repeated many times to determine the most critical location. Therefore, the numerical technique that can provide high efficiency has a huge advantage. This numerical technique is applied in the calculation of conductor reaction in the current Thesis. Those reactions will be reversed to represent the force transmitted from the conductors to the towers.

1.2.3 The response of TL structures under tornado wind load

A large number of transmission line failures caused by tornadoes have been reported in many places around the world. Ontario Hydro reported that five out of six right-of-way transmission line failures were caused by tornadoes within a 12-year period (Anders et al., 1984). In 2018, the tornado that hit Ottawa caused significant damage to the transmission system and impacted over 507000 customers (HydroOne, 2018). The tornado event that stroked Joplin caused regional damage to the transmission line system, resulting in power loss to over 20000 customers (Kuligowski et al., 2014). About 4000 poles and transmission towers were damaged under those tornadoes. China also experienced multiple transmission tower failures caused by tornadoes (Zhang, 2006, Xie and Zhu, 2011).

Triggered by the failure events, multiple studies have been conducted in the literature to estimate the response of transmission line structure under tornadoes. Carrington and White (2002) discussed the transmission tower failure and concluded that if the tornado failure containment is considered in the line design process, the cascading failure of the towers can be avoided. Oswald et al. (1994) analyzed several transmission line structural failures caused by multiple tornado strikes in the USA. They stated that longitudinal forces could be an important source of transmission failure. Hamada and Damatty (2016) studied the effect of different conductor parameters on longitudinal reactions. They also recommended considering cable force during the design process of towers subjected to tornado load.

Hamada et al. (2010) estimated the reaction of TL structures under tornado wind load based on the tornado simulation developed by Hangan and Kim (2008). They studied the response of the TL system under both F4 and F2 tornadoes, and mainly focused on guyed towers. Altalmas and El Damatty (2014) studied the response of simply supported TL towers under tornadoes, and also estimated the effect of different tornado positions on the tower member reactions. Hamada and El Damatty (2011) studied the conductor reaction under a tornado and tested the effect of tornado position on the conductor reactions. El Damatty and Hamada (2016) established critical F2 tornado wind load cases on transmission line systems. They considered an extensive range of tornado positions and proposed several critical tornado configurations. Those load cases were then simplified by El Damatty and Hamada (2015), which were later incorporated in the latest version of ASCE-74 (2020). Those load cases provide vertical profiles for the horizontal velocity acting on transmission towers, as well as a equivalent uniformly distributed loads acting on conductors. Alipour et al. (2020) proposed an analytical approach for calculating the response on a transmission tower subjected to tornado loading.

1.3 Objectives of Thesis

This Thesis mainly focuses on the response of transmission line conductors under tornado wind load. The major objectives of the Thesis can be summarized as follows:

1. Identify the critical tornado wind field and the corresponding critical position of the tornado center which can be used to design transmission lines to resist tornado wind loads.
2. Assess the effect of different conductor parameters on the longitudinal forces transferred from the conductors to the towers.
3. Develop a simple and yet accurate approach that can be used to estimate the peak conductor longitudinal forces, which can be used to design the towers to resist tornadoes.

1.4 Scope of Thesis

This Thesis is organized following the "Integrated Article" format. The current Chapter provided a review of the previous tornado and transmission lines under tornado studies, the objectives as well as the scope of the Thesis. The following Chapters address the objectives as presented below:

Chapter 2 – Response of transmission line conductors under different tornadoes

Multiple studies conducted in the past evaluated the conductor response under one tornado wind field, while the performance of transmission lines under different tornado wind fields still remains unknown. Thus, the objective of this Chapter is to estimate the variation in the conductor's critical longitudinal and transverse reactions under different tornado wind fields, as well as providing the corresponding critical tornado configurations. The considered full-scale tornadoes are the Spencer, South Dakota, 1998, the Stockton, Kansas, 2005 and the Goshen County, Wyoming, 2009. Computational Fluid Dynamics (CFD) simulations were previously conducted to develop these wind fields. All tornadoes have been rescaled to have a common velocity matching the upper limit of the F2 Fujita scale. Eight conductor systems, each including six spans, are considered in this Chapter. For each conductor, parametric studies are conducted by varying the location of the three tornado wind fields relative to the tower of interest, therefore the peak reactions associated with each tornado are determined. A semi-analytical closed-form solution previously developed and validated is used to calculate the reactions. The study conducted in this Chapter can be divided into two parts: In the first part, a parametric study considering a wide range of tornado locations is conducted. In the second part, the parametric study focuses on the tornado location leading to the critical tangential velocity on the tower. Based on this extensive parametric study, a critical tornado and its critical locations are recommended for design purposes.

Chapter 3 – Longitudinal reaction on conductors due to tornado wind load

The objective of this Chapter is to provide a set of charts that can be easily used to estimate the peak longitudinal forces transferred from the conductors to a tower. The wind field

considered in this Chapter is based on the tornado type and configurations determined from the previous Chapter. The charts should account for all the conductor parameters that can affect the value of the longitudinal force. In order to achieve that, a parametric study is first conducted to assess the variation of the longitudinal forces with different conductor parameters, based on the critical tornado configuration determined in the previous Chapter. Results of this parametric study are used to develop the charts that can be used to calculate longitudinal forces by adopting a multi-variable line regression. The forces calculated from charts are validated by finite element analysis. An example for the usage of the charts is provided at the end of this Chapter.

The last chapter of this Thesis presents the conclusions drawn from the two conducted studies and recommendations for future work.

1.5 The main contribution of this Thesis

By employing the numerical technique and tornado wind fields mentioned in the previous sections, the current Thesis estimated the critical tornado design parameters account for multiple tornado wind fields. The current state of knowledge in the field of tornado loads on conductors mainly focuses on a single tornado wind field, while a study that compares the conductor forces under different tornadoes still lacks in the literature. Also, the current study first proposed a simple and yet accurate approach to quickly calculate the conductor's critical longitudinal force under tornado wind load accounting for the conductor's actual parameters and multiple tornado configurations. Such an approach is simple enough to be applied by hand calculation, and yet shows good agreement in terms of predicting longitudinal forces when compared with finite element analysis.

1.6 Reference

Aboshosha, H. & A. El Damatty (2014) Effective technique to analyze transmission line conductors under high intensity winds. *Wind and Structures,* 18**,** 235-252.

Alipour, A., P. Sarkar, S. Dikshit, A. Razavi & M. Jafari (2020) Analytical Approach to Characterize Tornado-Induced Loads on Lattice Structures. *Journal of Structural Engineering,* 146**,** 04020108.

Altalmas, A. & A. A. El Damatty (2014) Finite element modelling of self-supported transmission lines under tornado loading. *Wind & structures,* 18**,** 473-495.

American Meteorological Society, A. (2021) Tornado. *Climatology. Glossary of Meteorology*.

Anders, G. J., P. L. Dandero & E. E. Neudorf (1984) Computation of Frequency of Right-of-Way Losses Due to Tornadoes. *IEEE Power Engineering Review,* PER-4**,** 37-37.

ASCE. 2020. Guidelines for Electrical Transmission Line Structural Loading. American Society of Civil Engineers Reston, VA.

Cao, Z. & H. Cai (2011) Detection of tornado frequency trend over Ontario, Canada. *The Open Atmospheric Science Journal,* 5.

Carrington, R. J. & H. B. White. 2002. A Pragmatic View of Some Important Transmission Line Design Issues. In *Electrical Transmission in a New Age,* 427-436.

Computer and Structures, I. (2016) SAP2000 V.19. *CSI Analysis Reference Manual*.

Doswell Iii, C. A., H. E. Brooks & N. Dotzek (2009) On the implementation of the enhanced Fujita scale in the USA. *Atmospheric Research,* 93**,** 554-563.

El Damatty, A. & A. Hamada (2016) F2 tornado velocity profiles critical for transmission line structures. *Engineering Structures,* 106**,** 436-449.

El Damatty, A., M. Hamada & A. Hamada. 2015. Simplified F2-Tornado load cases for transmission line structures. In *14th International Conference on Wind Engineering, Porto Alegre, Brazil*.

El Damatty, A. A., N. Ezami & A. Hamada. 2018. Case study for behaviour of transmission line structures under full-scale flow field of Stockton, Kansas, 2005 tornado. In *Electrical Transmission and Substation Structures 2018: Dedicated to Strengthening our Critical Infrastructure*, 257-268. American Society of Civil Engineers Reston, VA.

Fujita, T. T. (1981) Tornadoes and downbursts in the context of generalized planetary scales. *Journal of the Atmospheric Sciences,* 38**,** 1511-1534.

Gerges, R. R. & A. El-Damatty. 2002. Large displacement analysis of curved beams. In *Proceeding of CSCE Conference, Montreal, QC, Canada, ST*.

Grasso, L. D. & W. R. Cotton (1995) Numerical simulation of a tornado vortex. *Journal of Atmospheric Sciences,* 52**,** 1192-1203.

Hamada, A., A. El Damatty, H. Hangan & A. Shehata (2010) Finite element modelling of transmission line structures under tornado wind loading. *Wind and Structures, An International Journal,* 13**,** 451.

Hamada, A. & A. A. El Damatty (2011) Behaviour of guyed transmission line structures under tornado wind loading. *Computers and Structures,* 89**,** 986-1003.

Hamada, A. & A. A. El Damatty (2016) Behaviour of transmission line conductors under tornado wind. *Wind and Structures, An International Journal,* 22**,** 369-391.

Hangan, H. & J. Kim (2008) Swirl ratio effects on tornado vortices in relation to the Fujita scale. *Wind and Structures An International Journal,* 11**,** 291-302.

Hong, H. P., Q. Huang, W. J. Jiang, Q. Tang & P. Jarrett (2021) Tornado wind hazard mapping and equivalent tornado design wind profile for Canada. *Structural Safety,* 91**,** 102078.

HydroOne (2018) Major Events Response Report.

Koziey, B. L. & F. A. Mirza (1994) Consistent curved beam element. *Computers & structures,* 51**,** 643-654.

Kuligowski, E. D., F. T. Lombardo, L. T. Phan, M. L. Levitan & D. P. Jorgensen (2014) Final report, National Institute of Standards and Technology (NIST) technical investigation of the May 22, 2011, tornado in Joplin, Missouri.

Lee, W.-C. & J. Wurman (2005) Diagnosed three-dimensional axisymmetric structure of the Mulhall tornado on 3 May 1999. *Journal of Atmospheric Sciences,* 62**,** 2373-2393.

Leslie, L. & R. Smith. 1982. Numerical studies of tornado structure and genesis. In *Intense Atmospheric Vortices*, 205-213. Springer.

Lewellen, W. S., D. C. Lewellen & R. I. Sykes (1997) Large-eddy simulation of a tornado's interaction with the surface. *Journal of the atmospheric sciences,* 54**,** 581-605.

McDonald, J. R., K. C. Mehta, D. A. Smith & J. A. Womble. 2010. The enhanced Fujita scale: Development and implementation. In *Forensic Engineering 2009: Pathology of the Built Environment*, 719-728.

Minor, J. E., J. R. McDonald & K. C. Mehta (1993) The tornado: An engineering-oriented perspective.

Newark, M. J. (1984) Canadian tornadoes, 1950–1979. *Atmosphere-Ocean,* 22**,** 343-353.

Oswald, B., D. Schroeder, P. Catchpole, R. Carrington & B. Eisinger. 1994. Investigative summary of the July 1993 Nebraska Public Power District Grand Island-Moore 345 kV transmission line failure. In *Proceedings of IEEE/PES Transmission and Distribution Conference*, 574-580.

Potter, S. (2007) Fine-Tuning Fujita: After 35 years, a new scale for rating tornadoes takes effect. *Weatherwise,* 60**,** 64-71.

Refan, M., H. Hangan & J. Wurman (2014) Reproducing tornadoes in laboratory using proper scaling. *Journal of Wind Engineering and Industrial Aerodynamics,* 135**,** 136-148.

Rotunno, R. (1977) Numerical simulation of a laboratory vortex. *Journal of Atmospheric Sciences,* 34**,** 1942-1956.

Sarkar, P., F. Haan, W. Gallus Jr, K. Le & J. Wurman. 2005. Velocity measurements in a laboratory tornado simulator and their comparison with numerical and full-scale data. In *Proceedings of the 37th Joint Meeting Panel on Wind and Seismic Effects, Tsukuba, Japan, May*.

Shehata, A., A. El Damatty & E. Savory (2005) Finite element modeling of transmission line under downburst wind loading. *Finite Elements in Analysis and Design* 42**,** 71-89.

Twisdale, L. A. (1982) Wind-loading underestimate in transmission line design. *Transmission and Distribution***,** 40-46.

Wakimoto, R. M., N. T. Atkins & J. Wurman (2011) The LaGrange tornado during VORTEX2. Part I: Photogrammetric analysis of the tornado combined with single-Doppler radar data. *Monthly weather review,* 139**,** 2233-2258.

Wilson, T. & R. Rotunno (1986) Numerical simulation of a laminar end-wall vortex and boundary layer. *The Physics of fluids,* 29**,** 3993-4005.

Wurman, J. 2001. The DOW mobile multiple Doppler network. In *Preprints, 30th Int. Conf. on Radar Meteorology, Munich, Germany, Amer. Meteor. Soc*, 97.

Wurman, J. & C. R. Alexander (2005) The 30 May 1998 Spencer, South Dakota, storm. Part II: Comparison of observed damage and radar-derived winds in the tornadoes. *Monthly weather review,* 133**,** 97-119.

Wurman, J., J. Straka, E. Rasmussen, M. Randall & A. Zahrai (1997) Design and Deployment of a Portable, Pencil-Beam, Pulsed, 3-cm Doppler Radar. *Journal of Atmospheric and Oceanic Technology,* 14**,** 1502-1512.

Xia, J. 2001. *Large-eddy simulation of a three-dimensional compressible tornado vortex*. West Virginia University.

Xie, Q. & R. Zhu (2011) Earth, Wind, and Ice. *IEEE Power and Energy Magazine,* 9**,** 28-36.

Zhang, Y. (2006) Status quo of wind hazard prevention for transmission lines and countermeasures. *East China Electric Power,* 34**,** 28-31.

Chapter 2

2 Response of transmission line conductors under different tornadoes

2.1 Introduction

Transmission line structures play an essential role in transmitting electricity from the source of production to the users. Failure of transmission lines may cause an extensive range of power outages, resulting in severe economic losses and social distress. Localized strong wind events in the form of tornadoes, outbreaks and micro storms are called high intensity wind (HIW) events. It is believed that such incidents are responsible for more than 80% of all weather-related transmission line failures worldwide (Dempsey and White, 1996). Multiple transmission line structure failures related to HIWs were reported around the world. In 2011, an F2 tornado led to the collapse of five transmission towers in Sarnia, Ontario, Canada (Altalmas and El Damatty, 2014). In 2005, a tornado event in Hubei, China, caused 22 transmission line tower failures (Zhang, 2006). Triggered by the past failures, an extensive research program was conducted at the University of Western Ontario (UWO), Canada, to study the behavior of transmission line structures under tornado loading. As part of this program, the current study focuses on assessing the response of conductors under different tornado wind fields.

Tornadoes are short-lived localized surface vortices caused by thunderstorms. Fujita and Pearson (1973) defined a tornado as a highly convergent swirling wind affecting a relatively narrow path. In the scale proposed by Fujita (1981), tornadoes are divided into five categories based on the wind speed, path length, path width and frequencies. The smallest scale is F0, and the largest is F5. The current study is confined to F2 tornadoes, as it is reported in the ASCE-74 (2020), that 86% of the tornadoes measured in the United States have a scale of F2 or less. The current study is conducted numerically employing three different simulated tornado wind fields. The first tornado was developed by Hangan and Kim (2008) using a computational fluid dynamics (CFD) simulation, which was validated using field measurements recorded for the 1998 Spencer South Dakota F4 tornado by Wurman (1998). Hamada et al. (2010) developed an approach to scale-down

the CFD data to represent an F2 tornado. In this study, this tornado is referred to as the Design Tornado. The other two tornado wind fields were developed by El Damatty et al. (2018) based on the full-scale data collected from the Stockton, Kansas USA 2005 (STV1) tornado and Goshen County, Wyoming USA 2009 (GCV1) tornado using Doppler radars. The full-scale data were first analyzed by Refan et al. (2014), who summarized the flow pattern and the maximum velocity components of each tornado wind field.

A few studies were conducted to investigate the response of transmission line systems under tornadoes. Ishac and White (1994) discussed the effect of tornado loads on transmission lines. Savory (2001) modeled a self-supported lattice tower numerically and studied its failure under tornado wind load. Wang and Lv (2017) studied the response of a single transmission tower under a CFD simulated tornado wind field and compared it with the results calculated using the Chinese design guideline "110kV~750kV overhead transmission line design code" (GB 50545-2010). Only an isolated tower was considered in the two above-mentioned studies, without the inclusion of the conductors. The research program conducted at UWO on the effect of HIW on transmission line structures started by considering downbursts through the numerical model developed by Shehata et al. (2005). This numerical model, developed in-house, combined finite element simulations of all components of a line together with a representation of the wind field based on a CFD simulation. The tower members were simulated using three-dimensional finite elements, which the conductors and ground wires were simulated using two-dimensional curved frame elements developed by Gerges and El Damatty (2002). This numerical model was modified by Hamada et al. (2010) in order to analyze transmission lines under tornadoes. The two major modifications are the inclusion of a tornado wind field, based on the CFD simulation conducted by Hangan and Kim (2008), and the replacement of the two-dimensional line element used to model the conductors, with three-dimensional cable elements. The second modification was necessary because of the three-dimensional nature of the tornadoes and the presence of a significant vertical component compared to downbursts. The concept of conducting a parametric study by moving the tornado in space relative to the tower of interest was introduced in this study. The UWO research group used this model in a number of studies. The behaviour of guyed transmission towers under tornadoes was studied by Hamada and El Damatty (2011) and then the failure modes of

the same system were investigated by Hamada and El Damatty (2015). Altalmas and El Damatty (2014) studied the behaviour of simply supported transmission towers under tornadoes. A study focusing on determining the critical tornado location that maximizes the forces transferred from the conductors to the tower of interest was conducted by Hamada et al. (2016). The research at UWO led to the development of load cases simulating the critical effect of tornadoes on a generic transmission tower (Hamada and El Damatty, 2016). Those load cases were simplified by El Damatty et al.(2015) and were incorporated into the recent version of the ASCE-74 (2020) guidelines for transmission line loads. The above studies conducted at UWO were all based on the Design Tornado mentioned earlier in this section.

Since all the studies previously conducted at UWO employed only one tornado (Design Tornado), there is a need to assess the performance of transmission lines under different tornado fields. The availability of multiple tornado fields through the combination of field measurements and CFD currently enables conducting this assessment. Regardless of their magnitudes, the tornado structure might vary for various tornadoes. The current study focuses on assessing the conductor's behaviour under various tornadoes, and more specifically, the longitudinal and transverse forces transferred from the conductors to the tower of interest.

Two tornadoes are considered in this study together with the Design Tornado. The objective is to assess how much is the variation in the conductor’s peak reactions under different tornadoes. The reverse of those reactions represents the forces transferred from the conductors to the tower. The study considers a number of conductors, and for each conductor, parametric studies are conducted by varying the location of the three tornadoes relative to the tower of interest to determine the peak reactions associated with each tornado. Comparisons are carried out between those peak values. The specific objective is to assess if the Design Tornado provides conservative estimates for the reactions, and if not, how much it underestimates those reactions compared to the other two tornadoes.

The Chapter starts by describing the three considered tornadoes including their vertical and horizontal profiles. The structural numerical model used in the study is then briefly

described and validated. The parametric study conducted using the three tornadoes is then presented, which consists of two parts: (a) parametric study considering a wide range of tornado locations, (b) parametric study focusing on tornado location associated with peak tangential velocity acting on the tower. The conclusion and recommendation drawn from the results of the parametric study are finally presented.

2.2 Tornado wind fields

There are in total three tornado wind fields considered in this study. All of them are previously developed using the computational fluid dynamic (CFD) technique. No time variation was considered in the simulations, which were conducted in a steady-state manner. The tornado wind fields have three velocity components, which are the tangential velocity (V_t), the radial velocity (V_r) and the axial (vertical) velocity (V_a). The profile of each velocity component profile is a function of the cylindrical coordinate system (r, θ, z) measured from the center of tornado. The tornado models are assumed to be axisymmetric, where the velocity profile is averaged along the circumference, therefore is reduced to two-dimensional models in cylindrical coordinates. Since most of the tornadoes in North America are classified as F2 or less, as stated in ASCE 2020, the current study mainly focuses on F2 tornadoes. Designing transmission lines to resist tornadoes stronger than F2 would be uneconomical and impractical. According to the Fujita scale (Fujita, 1981), the 3-second gust of the F2 tornadoes ranges between 52.8 m/s and 72 m/s. Scaling the wind field to the 3-second gust implies a full correlation of tornado turbulence along the conductor spans, which is a reasonable assumption, as stated by Home et al. (2008). The three considered tornado fields are scaled up to the maximum value of the Fujita scale for F2 tornadoes. As such, the maximum velocity in the wind field $V_{resultant,max}$ is given by:

$$V_{resultant,max} = \sqrt{(V_t^2 + V_r^2 + V_a^2)} = 72 \text{ m/s}$$

The factors that define the structure of a simulated tornado wind field are mainly the swirl ratio (s), the length scale (ls) and the velocity scale (vs). Similar steps are employed to obtain these parameters for tornado wind fields. At first, lab-scale CFD tornado simulations were developed by solving RANS equations corresponding to different swirl ratio that

varies from 0.1 to 1. Then, the numerical results were benchmarked based on experimental data with a fixed swirl ratio s = 0.28, as recommended by Hangan and Kim (2008). In order to obtain the swirl ratio and length scale that can best fit the simulation with full-scale tornado data, an analysis was made by matching two parameters, the radius of maximum tangential velocity r_{max} and the height of maximum tangential velocity r_{max} of the real tornado. Such a process was repeated for all different swirl ratios, until for one specific s, the two length scales $r_{max,real}$ / $r_{max,CFD}$ and $z_{max,\ real}$ / $z_{max,\ CFD}$ converged. The corresponding swirl ratio and length scales are the proper parameters for the simulation. An example of this step is presented in Figure 2-1, which is based on the STV1 tornado simulation developed by El Damatty et al. (2018). The geometric length scale and corresponding swirl ratio are 3793 and 0.7, respectively based on their analysis. The final step was to obtain the velocity scale, which was accomplished by comparing the maximum tangential velocity obtained from full-scale data and the numerical simulation. For example, the velocity scale for the STV1 tornado was $\frac{V_{tn,max,real}}{V_{tn,max,lab-scale}} = \frac{50.2\ (m/s)}{2.013(m/s)} = 24.94$. The parameters for the Design Tornado are s = 1, ls = 4000 and vs = 13. The parameters for the CGV1 tornado are s = 1, ls = 1120 and vs = 19.3. The full-scale data are scaled-up in this study to the maximum 3-s gust velocity for F2 tornado as described earlier in this section. More details of the tornado simulations can be found at Hangan and Kim (2008), Hamada et al. (2010) and El Damatty et al. (2018). Table 2-1 presents the parameters of different tornado wind fields after scaling-up the wind field to the maximum velocity of F2 tornadoes.

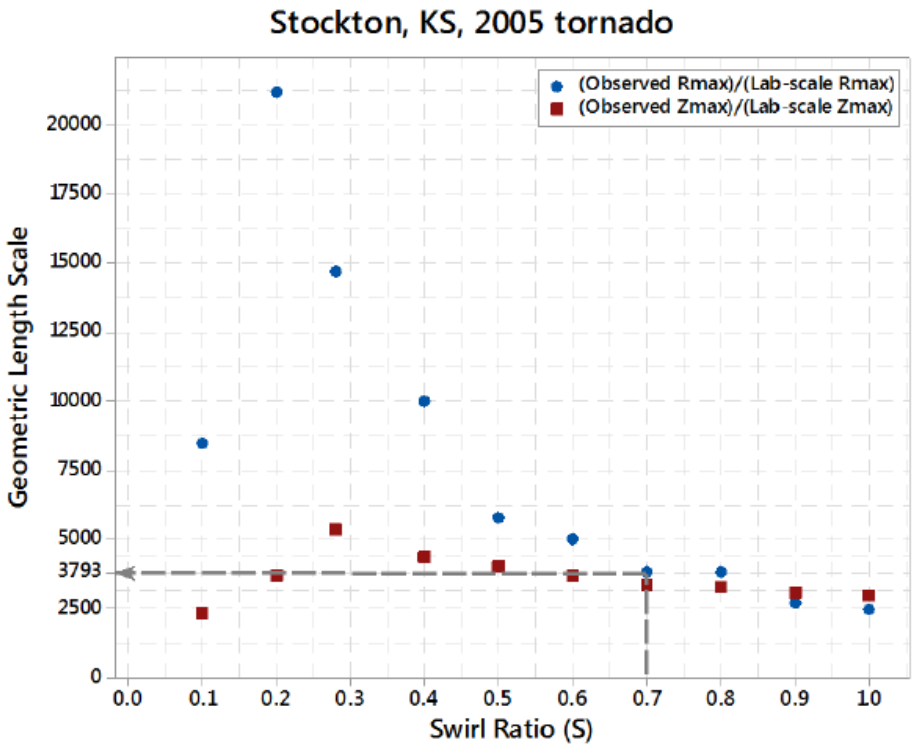

Figure 2-1 Geometric length scale of Stockton, KS, 2005 tornado for various swirl ratios (El Damatty et al. 2018)

Table 2-1 Parameters used in different tornado simulations

Tornado	**Corresponding swirl ratio (s)**	**Corresponding length scale (ls)**	**Corresponding velocity scale (vs)**
Design Tornado	1.0	4000	11.3
STV1	0.7	3793	32.4
GCV1	1.0	1120	31.8

After scaling into the F2 category, for the near ground height level (under 100 m), the maximum tangential velocity of the Design tornado is 69 m/s, occurring at a radius r = 96 m and height z = 19 m. The maximum radial velocity is 43 m/s which occurs at a radius r = 146 m and a height z = 6 m. Finally, the maximum axial velocity is 33 m/s which occurs

at a radius r = 171 m and a height z = 100 m. The maximum tangential velocity of the STV1 tornado is 65m/s, which occurs at a radius r = 225 m and a height z = 39 m. Next, the maximum radial velocity is 44 m/s which occurs at a radius r = 250 m and a height z = 9 m. Finally, the maximum axial velocity is 34 m/s which occurs at a radius r = 176 m and a height z = 52 m. The maximum tangential velocity of the GCV1 tornado is 69m/s, which occurs at a radius r = 148 m and a height z = 42 m. The maximum radial velocity is 45 m/s which occurs at a radius r = 174 m and a height z = 5 m. The maximum axial velocity is 28 m/s which occurs at a radius r = 125 m and a height z = 49 m.

Figure 2-2 presents the maximum velocity vertical profiles (under 100 m height) for three tornado wind fields. From the figure, it can be seen that the peak value of tangential velocity of Design Tornado occurs at a lower height level than the other two tornadoes. Both three tornadoes show similar behaviour when it comes to the peak radial velocity profile. As for axial velocity, the peak value of STV1 and GCV1 tornado occurs at around 40 m, and then the value of axial velocity decreases as height increases. The axial velocity for the Design Tornado keeps on increasing as height increases and reaches the maximum at 100 m height.

Figure 2-3 presents the transverse velocity distribution along conductor spans when the distance between the tornado center and the tower of interest is the radius $r_{tn,max}$ where the maximum tangential velocity occurs for three tornadoes. The transverse velocity results from the resolution of both the tangential and the radial components. The θ is determined to be 0° while the conductor height is the height where the peak value of tangential velocity occurs. Different tornado wind field provides different velocity distribution.

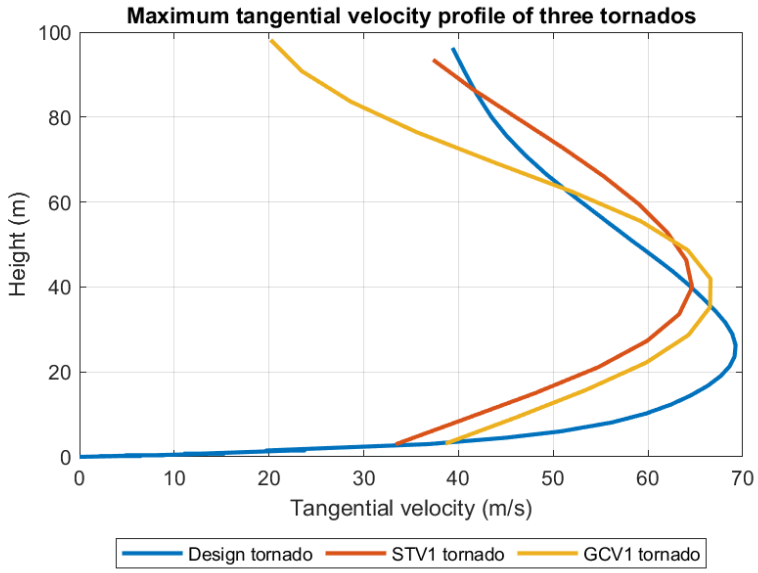
Maximum tangential velocity profile of three tornados
Height (m)
Tangential velocity (m/s)
Design tornado
STV1 tornado
GCV1 tornado

(a)

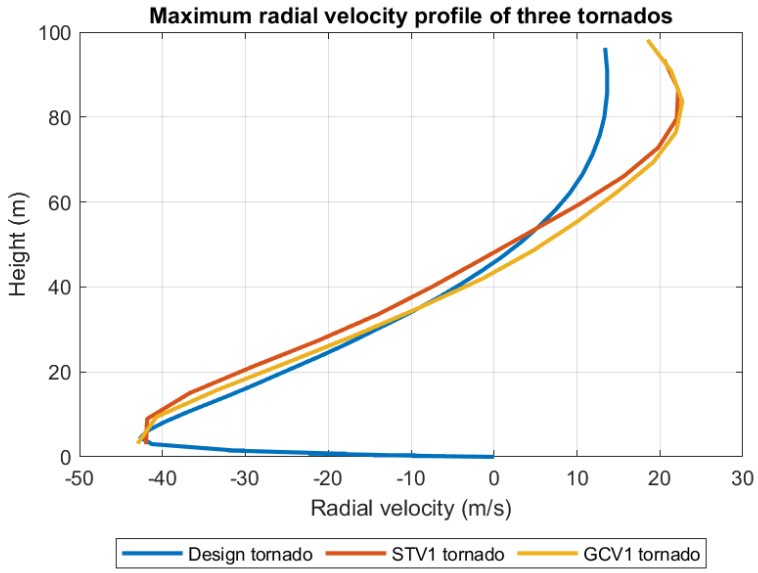
Maximum radial velocity profile of three tornados
Height (m)
Radial velocity (m/s)
Design tornado
STV1 tornado
GCV1 tornado

(b)

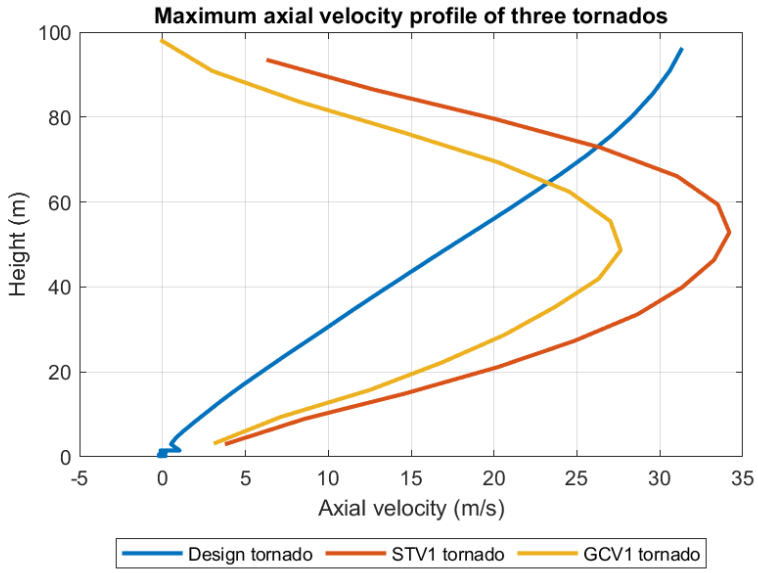

(c)

Figure 2-2 Maximum velocity profiles of three tornadoes (a) Tangential velocity (b) Radial velocity (c) Axial velocity

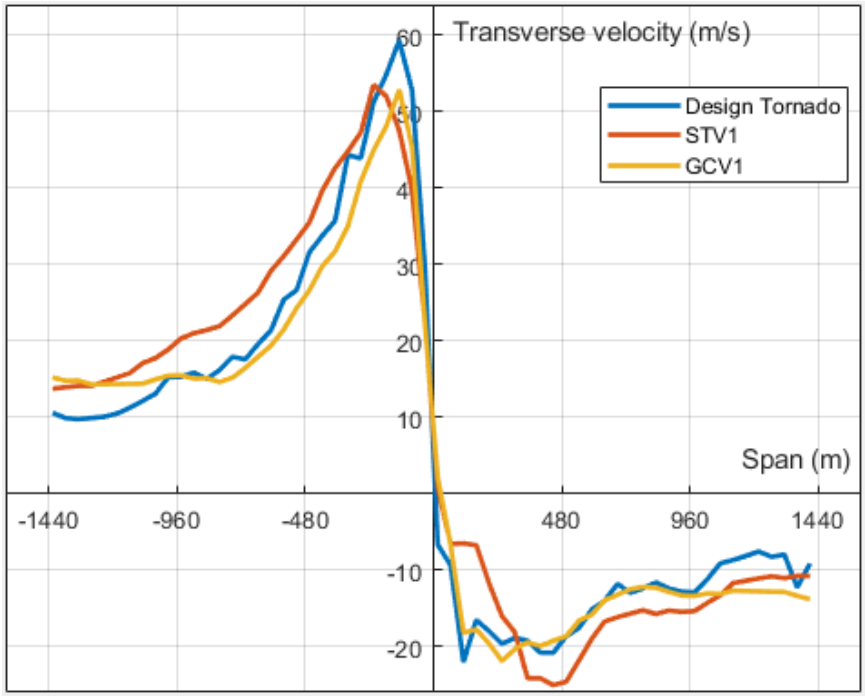

Figure 2-3 Tangential velocity distribution along conductor span at $R_{tan,max}$ and $\theta = 0°$ for three tornadoes

2.3 Modeling of the transmission line system

2.3.1 Conductor semi-analytical technique

In the current study, a semi-analytical technique developed and validated by Aboshosha and El Damatty (2014) is used to calculate the force transmitted from the conductors to the tower of interest under tornado wind load. Figure 2-4 presents the conductor system of this semi-analytical technique, which includes six spans of conductors, five insulators modeled as rigid pendulums with length h, and the corresponding boundary conditions. The selection of the number of spans is recommended by Shehata et al. (2005), who concluded that six spans are enough to provide an accurate prediction of the reactions at the middle tower. This technique can evaluate both longitudinal and transverse reactions generated on the conductors. The moment equilibrium is applied on conductor end points as well as hanging point of insulator, which leads to six non-linear equations with six unknowns. Those equations are then solved iteratively to obtain the reactions. This technique takes into account the pretension forces, the large deformation of the cable, as well as the flexibility of the insulators, which has a sufficient effect on the conductor's behaviour as indicated by Darwish et al. (2010). The main advantage of the semi-analytical technique compared to standard finite element analysis is its high efficiency, as it is 185 times faster than the finite element analysis. More details of the technique can be found at Aboshosha and El Damatty (2014).

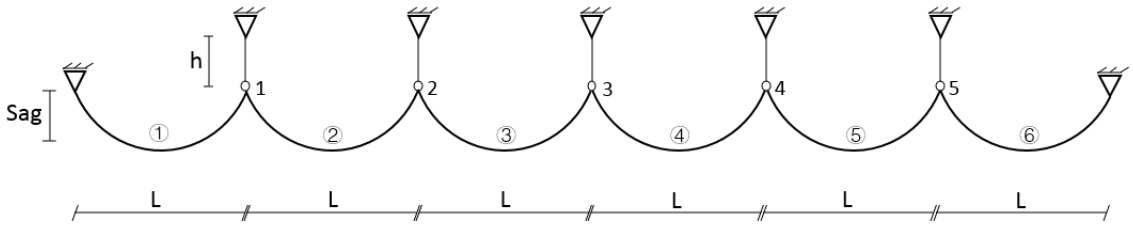

Figure 2-4 Conductor system presented by Aboshosha and El Damatty (2014)

2.3.2 Steps of analysis

The analysis regarding the conductor’s behaviour under tornado wind loads is conducted in the following steps:

(1) The tornado distance R and angle θ relative to the tower of interest is first determined, as presented in Figure 2-5 (a).

(2) The tornado velocity components corresponding to the selected location are applied to the conductor.

(3) The transverse velocity resulting from the tornado wind field then is determined based on the tangential and radial velocity components V_{tn} and V_{rd}, by applying the following equation: $V_{transverse} = V_{rd} * \cos(\beta) + V_{tn} * \cos(\beta + 90°)$. β represents the angle between the transverse direction and the line connecting the tornado center and the nodal point of conductor to which the transverse velocity is applied. Figure 2-5 (b) presents the layout for $V_{transverse}$, V_{tn}, V_{rd} and β.

(4) The semi-analytical technique is used to calculate the conductor's reactions in the longitudinal and transverse direction, based on the tornado's axial velocity components and the transverse velocity provided in the previous step. The conductor's longitudinal reaction Rx and transverse reaction Ry that will be transferred to the tower of interest are presented in Figure 2-5 (c).

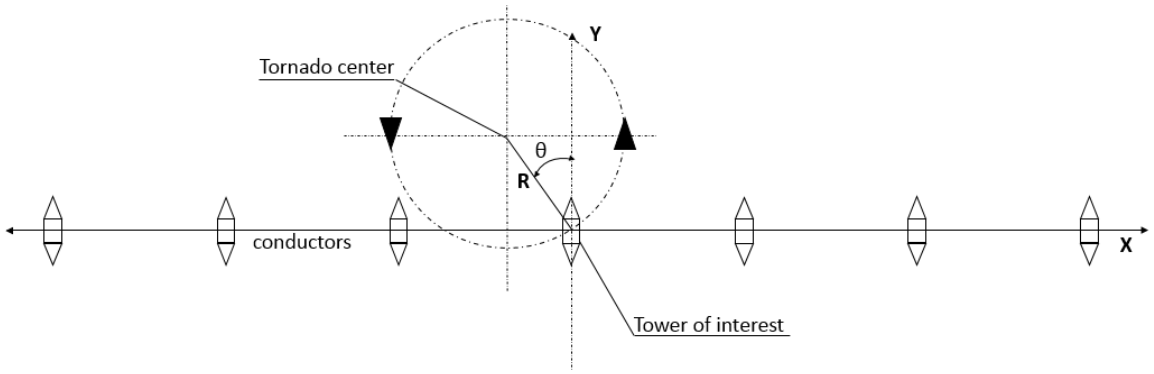

(a)

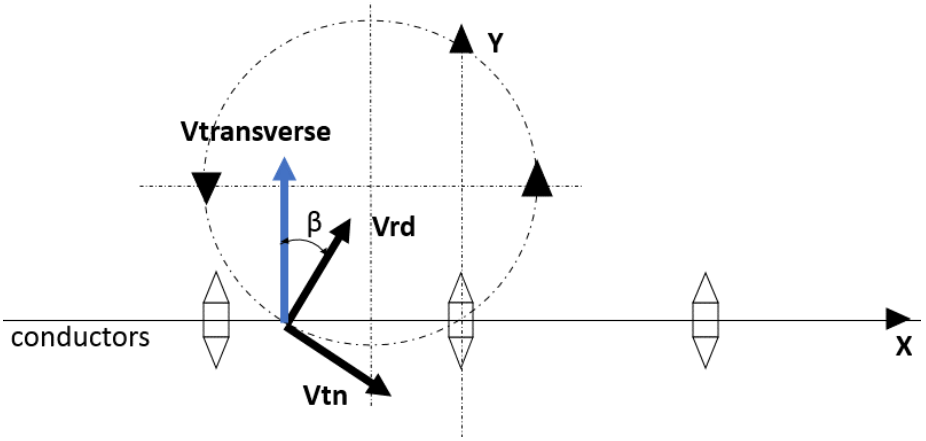

(b)

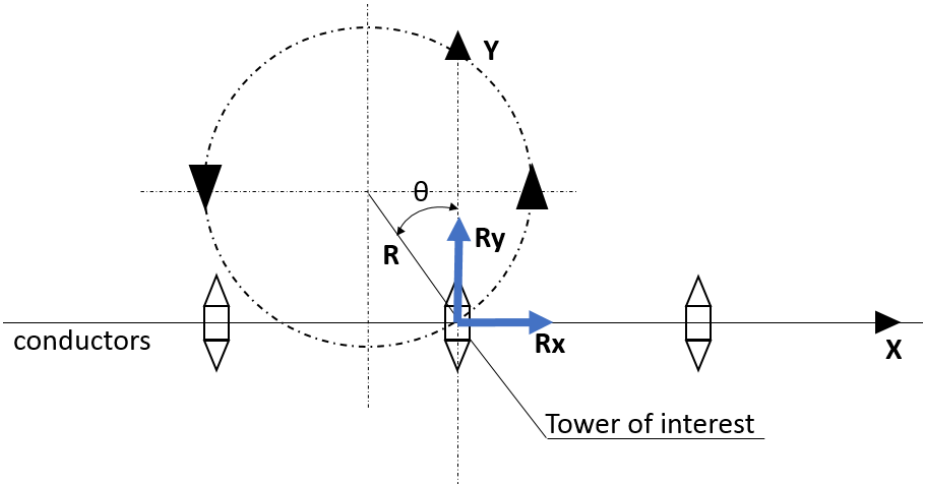

(c)

Figure 2-5 Layout for analysis (a) The location of Tornado (b) The transverse velocity acting on conductors (c) The longitudinal and transverse reaction

2.3.3 Validation of the technique

A comparison is made between the longitudinal reaction obtained by numerical technique and SAP2000 (CSI, 2016). A conductor with the same parameters is developed using both methods, and multiple tornado positions for the Design Tornado are chosen to provide the wind load. One of the tornado configurations, R = 125 m and θ = 0°, is presented in Figure 2-6. The conductor parameters are provided in Table 2-2. The chosen tornado positions and the results of the comparison are provided in Table 2-3, where the forces calculated by numerical technique and the SAP2000 are very close.

Table 2-2 Conductor parameters for comparison between numerical technique and SAP2000

Conductor Span L (m)	480
Conductor Weight w (N/m)	28.97
Conductor Diameter d_p (m)	0.04064
Insulator length h (m)	4.27
Sag (m)	20
Modulus of elasticity (N/m2)	6.23E+10
Conductor height (m)	33.96

Table 2-3 The results of comparison between numerical technique and SAP2000

Tornado position R (m), θ (°)	Numerical Result (N)	SAP2000 Result (N)	Difference
125, 0	7829	7902	0.92%
75, 15	6426	6363	-0.99%
175, 120	5548	5532	-0.29%

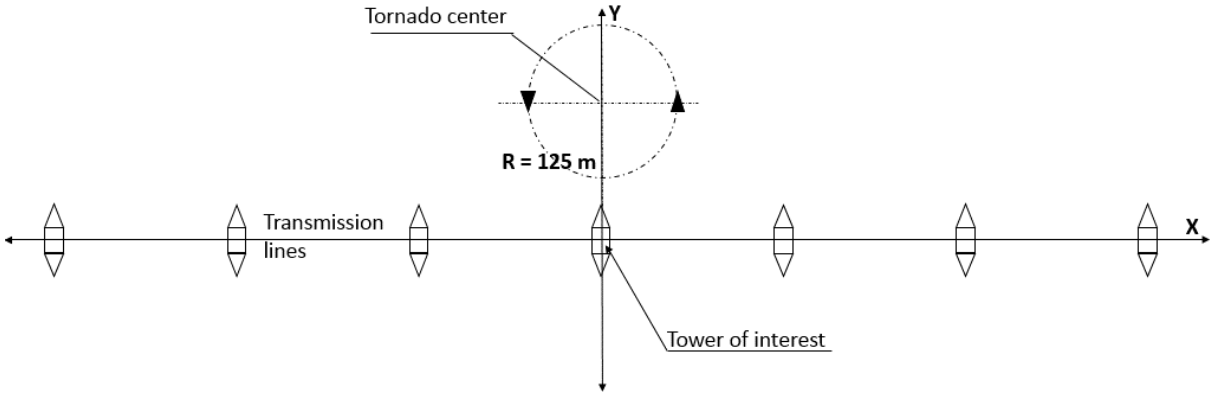

Figure 2-6 Schematic diagram of tornado configuration R = 125 m and θ = 0 °.

2.3.4 Validation of the required number of spans

In this part, multiple analyses are conducted to assess the appropriation of using three spans from each side of the tower of interest. The study is conducted by varying the number of spans and assessing the convergence of the longitudinal reaction at the middle tower. The tornado configurations used in this part of the study are R = 125 m and θ = 15°. The conductor parameters used in the analysis are provided in Table 2-4. The variation of the reaction Rx with the number of spans is presented in Figure 2-7, showing a convergent behaviour and indicating that six spans are suitable for an accurate estimation of R_x.

Table 2-4 The conductor parameters for validation

Conductor number	Span length(m)	Weight per unit length(m)	Conductor diameter(m)	Insulator length(m)	Sag(m)	Elastic modulus (m2/s)
N1	400	7.98	0.02159	4.27	16	6.48E10
N2	460	8.67	0.03259	4.27	14	5.18E10
N3	420	32.8	0.0527	4.9	15	7.03E10
N4	350	28.97	0.04064	4.27	10.5	6.23E10

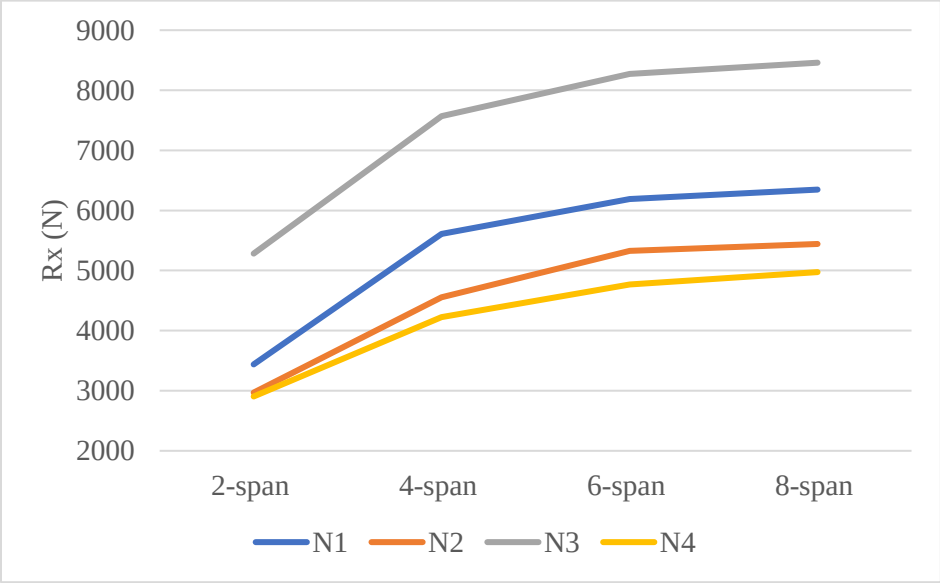

Figure 2-7 The reactions of different span number

2.4 Parametric study to determine critical design parameters

The three tornado wind fields and the previously described numerical model are used to conduct an extensive parametric study in order to determine the parameters leading to peak longitudinal and transverse reactions transferred from the conductors to the subject tower. Those parameters are:

(1) The most critical tornado among the three considered tornadoes
(2) The critical height of the conductors
(3) The critical tornado location defined by cylindrical coordinates R and θ

The parametric study is conducted by following the steps below:

(1) The selected conductors are simulated using the semi-analytical model.
(2) A tornado wind field is selected among the three considered tornadoes.
(3) A height, H, for the conductors is assumed within the practical range of values.
(4) A tornado location, defined by the cylindrical coordinates (R, θ), is assumed.
(5) Based on the tornado wind field and the assumed values of H, R and θ, the forces on the conductors are evaluated as described in section 2.3.2.
(6) The conductor is analyzed to obtain the reactions at the middle tower; the longitudinal reaction, Rx, and the transverse reactions, R_y.

Steps (1) to (6) are repeated for the eight considered conductors.

In the parametric study, the conductor heights ranged between 30 m and 60 m with an increment of 5 m. For each tornado, the radial distance between the tornado center and the middle tower varied between 75 m and 500 m, with an increment of 25 m. Meanwhile, the circumferential angel (θ) varied between 0° and 345°, with an increment of 15°. The presentation of the results was separated into two parts.

(1) Results for the entire range of R; Total Parametric Study Results.
(2) Results for the particular value of R corresponding to the peak vertical profiles on the tower; Peak Profile Results.

For each part, the results are presented for both the longitudinal and transverse reactions.

2.4.1 Conductor parameters

Eight different conductors are considered in conducting the extensive parametric study. The geometric and material properties of the conductors are provided in Table 2-5.

Table 2-5 Properties of conductors used in the parametric study

Conductor number	C1	C2	C3	C4	C5	C6	C7	C8
Span(m)	480	400	460	213.36	450	420	289.36	350
Weight(N/m)	28.97	7.98	8.67	28.97	20.14	32.8	17.92	28.97
Diameter(m)	0.04064	0.02159	0.02159	0.0345	0.034	0.0527	0.04	0.04064
Insulator length(m)	4.27	4.27	4.27	2.44	2.44	4.9	3.2	4.27
Sag(m)	20	16	14	3.9	19.5	15	8.5	10.5
Modulus of elasticity(N/m2)	6.23E+10	6.48E+10	5.18E+10	1.86E+11	6.48E+10	7.03E+10	6.23E+10	6.23E+10

2.5 Total Parametric Study Results

2.5.1 Longitudinal Reactions

Table 2-6 reports the peak longitudinal reactions obtained from the parametric study conducted for all the conductors, for all the considered heights and under the three considered tornadoes. The value reported in each cell represents the maximum reaction obtained as a result of moving the three considered tornadoes in space. The critical tornado corresponding to each peak value is reported in Table 2-7. The cylindrical coordinates of the tornado location associated with the peak values are reported in Table 2-9. As shown in Table 2-7, all the critical reactions result from the STV1 and the Design Tornado. One of the objectives of this study is to assess if the Design Tornado can be used to develop critical load cases for the design of transmission towers. As such, the percentage

differences between the maximum values obtained from the critical tornado, reported in Table 2-6, and the corresponding values obtained from the Design Tornado, are reported in Table 2-8. The maximum difference occurs at C1 with a height of 55 m, which is over 30 %. Except for C4 and C7, which have smaller span lengths, STV1 appears to be the critical tornado for the majority of cases. The critical height H is determined to be 50 m, which provides the minimum difference between the maximum Rx. Table 2-9 reports the tornado positions corresponding to the critical reactions, which shows that the tornado distance R associated with maximum longitudinal force varies as span length changes. When the span length has a smaller value, the critical R also decreases. In general, the critical R remains consistent with the span length. The critical θ is determined to be 90°. As such, the design parameters for longitudinal reaction can be: the Design Tornado and STV1 tornado, with H = 50 m, R equals to the span length, and θ = 90°.

Table 2-6 The maximum longitudinal reactions of each conductor under different heights.

Maximum longitudinal reaction(N)								
height(m)	C1	C2	C3	C4	C5	C6	C7	C8
30	8963	7042	5726	1860	12929	9770	7907	6165
35	9925	8740	7245	**1864**	13545	12401	8244	6994
40	12716	9620	8544	1843	17111	14464	8313	7264
45	14971	10074	**9241**	1834	20005	14897	**8384**	**7405**
50	15432	**10544**	9092	1721	**21501**	**15338**	8296	7155
55	**15856**	10356	9011	1676	21053	15120	8264	6677
60	15770	9673	8641	1656	20728	14214	8238	6751

Table 2-7 The critical tornado wind field of each conductor under different heights.

Tornado corresponding to the maximum longitudinal reaction								
height(m)	C1	C2	C3	C4	C5	C6	C7	C8
30	Design	STV1	STV1	Design	STV1	STV1	Design	STV1
35	STV1	STV1	STV1	Design	STV1	STV1	Design	STV1
40	STV1	STV1	STV1	STV1	STV1	STV1	Design	STV1
45	STV1	STV1	STV1	STV1	STV1	STV1	Design	STV1
50	STV1	STV1	STV1	Design	STV1	STV1	Design	STV1
55	STV1	STV1	STV1	Design	STV1	STV1	Design	Design
60	STV1	STV1	STV1	Design	STV1	STV1	Design	Design

Table 2-8 Difference of Rx between the Design Tornado and the critical tornado under total parametric study.

Difference between Rx from Design tornado and maximum longitudinal reaction under total parametric study								
height(m)	C1	C2	C3	C4	C5	C6	C7	C8
30	0.00%	-4.07%	-8.76%	0.00%	-1.99%	-7.15%	0.00%	-12.19%
35	-8.94%	-14.84%	-30.06%	0.00%	-4.64%	-24.46%	0.00%	-11.80%
40	-28.43%	-12.60%	-36.09%	-1.40%	-17.78%	-25.65%	0.00%	-13.82%
45	-33.31%	-12.09%	-41.12%	-3.27%	-21.92%	-26.34%	0.00%	-12.11%
50	-30.73%	-15.84%	-30.78%	0.00%	-28.45%	-26.63%	0.00%	-6.88%
55	-31.27%	-11.70%	-27.53%	0.00%	-21.84%	-20.75%	0.00%	0.00%
60	-25.02%	-3.48%	-19.14%	0.00%	-16.53%	-12.39%	0.00%	0.00%

Table 2-9 The critical tornado location for each conductor under different heights

Tornado location corresponding to maximum longitudinal reaction (R, θ) (m, °)								
height(m)	C1	C2	C3	C4	C5	C6	C7	C8
30	350, 225	400, 90	425, 90	225, 90	175, 15	400, 90	275, 90	350, 90
35	450, 90	400, 90	450, 90	225, 90	425, 90	425, 90	300, 90	350, 90
40	450, 90	425, 90	450, 90	325, 90	450, 90	425, 90	275, 90	350, 90
45	475, 90	425, 90	450, 90	325, 90	475, 90	425, 90	275, 90	350, 90
50	500, 90	425, 90	450, 90	250, 90	475, 90	425, 90	275, 90	375, 90
55	500, 90	425, 90	475, 90	250, 90	475, 90	425, 90	300, 90	350, 90
60	500, 90	425, 90	475, 90	275, 90	475, 90	425, 90	300, 90	350, 90

2.5.2 Transverse Reactions

Table 2-10 to Table 2-13 present the results for the transverse reactions with the same logic and sequence presented for the longitudinal reactions. For the transverse reaction, the STV1 tornado was the governing one for all the cases. The heights corresponding to maximum transverse reaction, H_{cr}, is determined to be 50 m, which provides the minimum difference between peak reaction for the conductors with different H_{cr}. As presented in Table 2-13, the tornado distance R leading to maximum transverse reaction varies from 275 m to 325 m, while the angle θ corresponding to peak value is 90° for all conductors. The R is determined to be 300 m as it also provides the minimum difference between peak reactions for conductors.

Table 2-12 presents the difference between Ry calculated from Design Tornado and the peak reaction, where the maximum difference is 18%. Therefore, the design parameters for transverse reaction can be: STV1 tornado, with H = 50 m, R = 300 m and θ = 90°

Table 2-10 The critical tornado wind field of each conductor under different heights.

Tornado corresponding to the maximum transverse reaction								
height(m)	C1	C2	C3	C4	C5	C6	C7	C8
30	STV1	STV1	STV1	STV1	STV1	STV1	STV1	STV1
35	STV1	STV1	STV1	STV1	STV1	STV1	STV1	STV1
40	STV1	STV1	STV1	STV1	STV1	STV1	STV1	STV1
45	STV1	STV1	STV1	STV1	STV1	STV1	STV1	STV1
50	STV1	STV1	STV1	STV1	STV1	STV1	STV1	STV1
55	STV1	STV1	STV1	STV1	STV1	STV1	STV1	STV1
60	STV1	STV1	STV1	STV1	STV1	STV1	STV1	STV1

Table 2-11 The maximum transverse reactions of each conductor under different heights.

Maximum transverse reaction(N)								
height(m)	C1	C2	C3	C4	C5	C6	C7	C8
30	23146	11632	12309	13758	19106	28633	18969	23146
35	23303	11797	12308	13904	19362	28982	**19265**	23303
40	23610	12034	12386	**14039**	19850	29166	19098	23610
45	23876	**12113**	12605	13897	20143	29625	19254	23876
50	**24284**	12101	**12641**	13597	20327	**29683**	19146	**24284**
55	24254	11875	12454	13097	**20360**	29112	18793	24254
60	23800	11587	12092	12684	19976	28163	18191	23800

Table 2-12 Difference between Ry from Design Tornado and maximum transverse reaction

Difference between Ry from Design Tornado and maximum transverse reaction								
height(m)	C1	C2	C3	C4	C5	C6	C7	C8
30	-5.32%	-6.06%	-8.46%	-8.16%	-4.52%	-6.66%	-8.29%	-6.04%
35	-8.64%	-9.57%	-10.37%	-10.85%	-8.69%	-10.42%	-10.28%	-9.92%
40	-11.19%	-12.28%	-13.18%	-12.29%	-11.97%	-12.52%	-11.55%	-13.49%
45	-13.74%	-15.15%	-16.73%	-11.73%	-15.45%	-16.13%	-13.28%	-13.67%
50	-17.10%	-14.97%	-18.04%	-11.10%	-16.99%	-16.32%	-12.63%	-12.58%
55	-17.55%	-13.65%	-17.07%	-7.28%	-17.14%	-15.36%	-11.91%	-10.23%
60	-17.14%	-11.85%	-15.79%	-3.61%	-16.47%	-13.11%	-8.56%	-8.84%

Table 2-13 The critical tornado distance of each conductor under different heights

Tornado location corresponding to maximum transverse reaction (R, θ) (m, °)								
height(m)	C1	C2	C3	C4	C5	C6	C7	C8
30	325, 60	275, 60	325, 60	275, 75	300, 60	325, 60	275, 75	325, 60
35	325, 60	300, 75	325, 75	275, 75	300, 75	300, 75	300, 75	325, 60
40	325, 75	300, 75	300, 90	250, 90	300, 75	300, 75	300, 90	325, 75
45	300, 90	275, 90	300, 90	250, 90	300, 90	300, 90	300, 90	300, 90
50	325, 90	300, 90	325, 90	275, 90	300, 90	300, 90	300, 90	325, 90
55	325, 90	300, 90	325, 90	275, 90	325, 90	300, 90	300, 90	325, 90
60	325, 90	300, 90	325, 90	275, 105	325, 90	300, 90	300, 90	325, 90

2.6 Peak Profile Results

The response of a transmission tower to tornadoes depends on the loads acting on the tower itself and the forces transferred from the conductors. The tornado locations leading to peak reactions obtained from the total parametric study do not correspond to the locations associated with the maximum vertical profile and, consequently, the location for maximum forces acting on the tower. As such, it is important to determine the peak reactions associated with the tornado location corresponding to maximum peak vertical profiles. Therefore, out of the total parametric study, the results are extracted for the tornado location corresponding to peak tangential velocity vertical profiles for each tornado and are presented in this subsection. Those locations, R_{max}, are 100 m for the Design Tornado, 225 m for the STV1 and 150 m for the GCV1. In order to be more accurate, extra locations close to those of maximum tangential velocities are considered, as provided in Table 2-14.

Table 2-14 R_{max} of three tornadoes used in the parametric study

Tornado	Design			STV1		GCV1		
Tornado distance R_{max}(m)	100	125	75	225	250	150	175	125
Maximum tangential velocity(m/s)	69	68	67.9	65.39	64.88	69.23	67.3	66.74
Height of peak(m)	26.28	34.3	14.42	39.9	46.3	41.9	41.92	35.3

2.6.1 Longitudinal results

The results for the considered reactions are presented in Table 2-15 to Table 2-18. It should be noted that the values reported in Table 2-15 are the peak values obtained from the three tornadoes after varying the angle θ while maintaining a fixed value of R. The results indicate that again the Design and STV1 tornadoes provide peak values for all cases, while the Design Tornado is more prevailing in this case.

Since the purpose is to develop design charts that can be applied to a general transmission line, the heights leading to peak reactions, H_{cr}, should be considered in the development of those charts. Table 2-15 shows that for all conductors, H_{cr} = 30 m except for C2, H_{cr} = 35 m. As such, those two values can be considered for design purposes.

The difference between the peak values reported in Table 2-15 and the corresponding values associated with the Design Tornado are provided in Table 2-17. Focusing on H = 30 m and H = 35 m (the critical heights), the difference will be less than 6.1%, which is small enough to justify the use of the Design Tornado for design purposes.

Table 2-18 presents the tornado position corresponding to the peak values. It shows that after determining H_{cr} = 35 m for C2 and H_{cr} = 30 m for all other conductors, the tornado distance leading to critical value is R = 125 m. When the tornado configuration is determined to be the Design Tornado with H_{cr} = 30 m or 35 m and R = 125 m, the angle θ leading to peak value is 30° for C4 and C7 while 15° for other conductors. Those two values can also be considered for design purposes. Therefore, for longitudinal reaction, the design parameters can be: Design Tornado, with H = 30 m or 35 m, R = 125 m and θ = 15° or 30°.

Table 2-15 The maximum longitudinal reactions of each conductor with different heights under R_{max}.

Maximum longitudinal reaction under R_{max} (N)								
height(m)	C1	C2	C3	C4	C5	C6	C7	C8
30	**8230**	6140	**5305**	**1324**	**12882**	**8070**	**6226**	**4766**
35	8169	**6152**	5092	1214	12683	7938	5839	4591
40	7828	5753	4612	1173	12438	7464	5500	4352
45	7263	5010	4085	1052	11475	6703	5007	4215
50	6651	4406	3606	868	10402	6032	4628	3894
55	6037	3781	3163	765	9413	5417	3920	3456
60	5567	3255	2661	677	8531	4802	2846	2905

Table 2-16 The critical tornado wind field of each conductor with different heights under R_{max}.

Tornado corresponding to the maximum longitudinal reaction under R_{max} (N)								
height(m)	C1	C2	C3	C4	C5	C6	C7	C8
30	STV1	Design	Design	Design	STV1	Design	Design	Design
35	Design	Design	Design	STV1	Design	Design	STV1	Design
40	Design	Design	Design	STV1	Design	Design	STV1	STV1
45	Design	Design	Design	STV1	Design	Design	STV1	STV1
50	Design	Design	Design	STV1	Design	Design	STV1	STV1
55	Design	Design	Design	Design	Design	Design	STV1	STV1
60	Design	Design	Design	Design	Design	Design	STV1	STV1

Table 2-17 Difference between Rx from Design tornado and maximum longitudinal reaction under R_{max}

Difference between Rx from Design tornado and maximum longitudinal reaction under R_{max}								
height(m)	C1	C2	C3	C4	C5	C6	C7	C8
30	-6.1%	0.0%	0.0%	0.0%	-4.5%	0.0%	0.0%	-6.1%
35	0.0%	0.0%	0.0%	-3.0%	0.0%	0.0%	-4.7%	0.0%
40	0.0%	0.0%	0.0%	-10.0%	0.0%	0.0%	-12.4%	0.0%
45	0.0%	0.0%	0.0%	-9.2%	0.0%	0.0%	-15.2%	0.0%
50	0.0%	0.0%	0.0%	-1.5%	0.0%	0.0%	-20.1%	0.0%
55	0.0%	0.0%	0.0%	0.0%	0.0%	0.0%	-21.1%	0.0%
60	0.0%	0.0%	0.0%	0.0%	0.0%	0.0%	-9.6%	0.0%

Table 2-18 The critical tornado location of each conductor with different heights under R_{max}

Tornado location corresponding to maximum longitudinal reaction under R_{max} (R, θ) (m, °)								
height(m)	C1	C2	C3	C4	C5	C6	C7	C8
30	225, 165	125, 15	125, 15	125, 30	225, 165	125, 15	125, 30	125, 15
35	125, 165	125, 15	125, 15	250, 90	125, 165	125, 15	250, 90	125, 30
40	125, 165	125, 15	125, 15	250, 90	125, 165	125, 15	250, 90	250, 90
45	125, 165	125, 15	125, 15	250, 90	125, 0	125, 15	250, 90	250, 90
50	125, 0	125, 15	125, 15	250, 105	125, 0	125, 15	250, 105	250, 105
55	125, 15	125, 15	125, 15	125, 45	125, 15	125, 15	250, 105	250, 105
60	125, 15	125, 15	125, 15	125, 45	125, 15	125, 15	250, 105	250, 105

2.6.2 Transverse results

The results for the transverse reactions are presented in Table 2-19 to Table 2-22. The results indicate that consistently the STV1 provides the peak transverse reactions. The results also show that for most of the cases, the critical height H_{cr} equals to 45 m. Two peak cases are associated with H = 40 m and one case corresponding to H = 50 m. However, the difference between those cases and the one corresponding to H = 45 m is small. With the exception of C1, the critical angle for all conductors is 90°, as presented in Table 2-22.

Table 2-21 shows that under Peak Profile Study, the difference between the transverse reaction provided by Design Tornado and the peak R_y becomes larger, where the maximum difference can reach 48.91%. As such, for transverse reactions, the design parameters can be: STV1 tornado, with H = 45 m, R = 225 m, and θ = 90°.

Table 2-19 The critical tornado wind field of each conductor with different heights under R_{max}.

Tornado corresponding to the maximum transverse reaction under R_{max}								
height(m)	C1	C2	C3	C4	C5	C6	C7	C8
30	STV1	STV1	STV1	STV1	STV1	STV1	STV1	STV1
35	STV1	STV1	STV1	STV1	STV1	STV1	STV1	STV1
40	STV1	STV1	STV1	STV1	STV1	STV1	STV1	STV1
45	STV1	STV1	STV1	STV1	STV1	STV1	STV1	STV1
50	STV1	STV1	STV1	STV1	STV1	STV1	STV1	STV1
55	STV1	STV1	STV1	STV1	STV1	STV1	STV1	STV1
60	STV1	STV1	STV1	STV1	STV1	STV1	STV1	STV1

Table 2-20 The maximum transverse reactions of each conductor with different heights under R_{max}.

Maximum transverse reaction under R_{max} (N)								
height(m)	C1	C2	C3	C4	C5	C6	C7	C8
30	22473	11455	11929	13726	18761	28024	18614	22473
35	22414	11528	11660	13845	18772	27966	18787	22414
40	22002	11726	11996	**14039**	18792	28576	**18880**	22002
45	**22618**	**11905**	**12113**	13897	19433	**28828**	18867	**22618**
50	22590	11806	11903	13521	**19446**	28537	18541	22590
55	22244	11502	11594	12939	19090	27755	17966	22244
60	21532	11034	11197	12526	18451	26679	17188	21532

Table 2-21 Difference between Ry from Design Tornado and maximum transverse reaction under $R_{max.}$

Difference between Ry from Design Tornado and maximum transverse reaction under R_{max}								
height(m)	C1	C2	C3	C4	C5	C6	C7	C8
30	-25.57%	-25.73%	-28.20%	-19.62%	-25.02%	-27.17%	-25.82%	-26.52%
35	-29.56%	-31.55%	-31.47%	-21.24%	-29.45%	-32.43%	-27.73%	-34.37%
40	-33.43%	-37.64%	-39.29%	-22.59%	-34.73%	-39.27%	-28.02%	-37.84%
45	-40.62%	-43.63%	-45.08%	-22.46%	-41.48%	-44.29%	-27.96%	-37.51%
50	-45.06%	-44.20%	-47.13%	-21.75%	-46.28%	-46.46%	-26.09%	-35.92%
55	-48.91%	-41.68%	-46.46%	-20.01%	-46.92%	-44.40%	-24.39%	-33.96%
60	-48.22%	-39.37%	-43.82%	-18.85%	-44.13%	-42.17%	-21.60%	-30.99%

Table 2-22 The critical tornado distance of each conductor with different heights under $R_{max.}$

Tornado location corresponding to maximum transverse reaction under R_{max} (R, θ) (m, °)								
height(m)	C1	C2	C3	C4	C5	C6	C7	C8
30	250, 60	250, 60	250, 60	250, 75	250, 60	250, 60	250, 75	250, 60
35	250, 60	250, 75	250, 75	250, 90	250, 60	250, 75	250, 75	250, 75
40	250, 75	250, 90	250, 90	250, 90	250, 90	250, 90	250, 90	250, 90
45	250, 90	250, 90	250, 90	250, 90	250, 90	250, 90	250, 90	250, 90
50	250, 90	250, 90	250, 90	250, 90	250, 90	250, 90	250, 90	250, 90
55	250, 90	250, 90	250, 90	250, 105	250, 90	250, 90	250, 90	250, 90
60	250, 90	250, 105	250, 105	250, 105	250, 90	250, 105	250, 105	250, 105

2.7 Conclusions

The following conclusions can be drawn from the conducted study:

For the Total Parametric Study results:

- For the longitudinal reaction, the critical parameters are: the Design Tornado and the STV1 tornado, with H = 50 m, R equals to the span length, and $\theta = 90°$.
- For the transverse reaction, the critical parameters are: the STV1 tornado, with H = 50 m, R = 300 m, and $\theta = 90°$.

For the Peak Profile Study results:

- For the longitudinal reaction, the critical parameters are: the Design Tornado, with H = 30 m or 35 m, R = 125 m, and $\theta = 15°$ or 30°.
- For the transverse reaction, the critical parameters are: the STV1 tornado, with H = 45 m, R = 250 m, and $\theta = 90°$

2.8 Acknowledgement

The authors gratefully acknowledge the Natural Sciences and Engineering Research Council of Canada (NSERC) and Hydro One Company for their kind financial support of this research.

2.9 References

Aboshosha, H. & A. El Damatty (2014) Effective technique to analyze transmission line conductors under high intensity winds. *Wind and Structures,* 18**,** 235-252.

Altalmas, A. & A. A. El Damatty (2014) Finite element modelling of self-supported transmission lines under tornado loading. *Wind & structures,* 18**,** 473-495.

ASCE. 2020. Guidelines for Electrical Transmission Line Structural Loading. American Society of Civil Engineers Reston, VA.

Computer and Structures, I. (2016) SAP2000 V.19. *CSI Analysis Reference Manual*.

Darwish, M. M., A. A. El Damatty & H. Hangan (2010) Dynamic characteristics of transmission line conductors and behaviour under turbulent downburst loading. *Wind and Structures,* 13**,** 327.

Dempsey, D. & H. White (1996) Winds wreak havoc on lines. *Transmission and Distribution World,* 48**,** 32-37.

El Damatty, A. & A. Hamada (2016) F2 tornado velocity profiles critical for transmission line structures. *Engineering Structures,* 106**,** 436-449.

El Damatty, A., M. Hamada & A. Hamada. 2015. Simplified F2-Tornado load cases for transmission line structures. In *14th International Conference on Wind Engineering, Porto Alegre, Brazil*.

El Damatty, A. A., N. Ezami & A. Hamada. 2018. Case study for behaviour of transmission line structures under full-scale flow field of Stockton, Kansas, 2005 tornado. In *Electrical Transmission and Substation Structures 2018: Dedicated to Strengthening our Critical Infrastructure*, 257-268. American Society of Civil Engineers Reston, VA.

Fujita, T. T. (1981) Tornadoes and downbursts in the context of generalized planetary scales. *Journal of the Atmospheric Sciences,* 38**,** 1511-1534.

Fujita, T. T. & A. D. Pearson. 1973. Results of FPP classification of 1971 and 1972 tornadoes. In *Eight conference on severe local storms*, 142-145.

GB50545-2010 (2010) Code for design of 110kV~750kV overhead transmission line.

Gerges, R. R. & A. El-Damatty. 2002. Large displacement analysis of curved beams. In *Proceeding of CSCE Conference, Montreal, QC, Canada, ST*.

Hamada, A. & A. A. El Damatty (2011) Behaviour of guyed transmission line structures under tornado wind loading. *Computers and Structures,* 89**,** 986-1003.

Hamada, A. & A. A. El Damatty (2015) Failure analysis of guyed transmission lines during F2 tornado event. *Engineering Structures,* 85**,** 11-25.

Hamada, A. & A. A. El Damatty (2016) Behaviour of transmission line conductors under tornado wind. *Wind and Structures, An International Journal,* 22**,** 369-391.

Hamada, A., A. El Damatty, H. Hangan & A. Shehata (2010) Finite element modelling of transmission line structures under tornado wind loading. *Wind and Structures, An International Journal,* 13**,** 451.

Hangan, H. & J. Kim (2008) Swirl ratio effects on tornado vortices in relation to the Fujita scale. *Wind and Structures An International Journal,* 11**,** 291-302.

Holmes, J. D., H. M. Hangan, J. Schroeder, C. Letchford & K. D. Orwig (2008) A forensic study of the Lubbock-Reese downdraft of 2002. *Wind and Structures An International Journal,* 11**,** 137-152.

Ishac, M. F. & H. B. White. 1994. Effect of tornado loads on transmission lines. In *Proceedings of IEEE/PES Transmission and Distribution Conference*, 521-527. IEEE.

Refan, M., H. Hangan & J. Wurman (2014) Reproducing tornadoes in laboratory using proper scaling. *Journal of Wind Engineering and Industrial Aerodynamics,* 135**,** 136-148.

Savory, E., G. A. Parke, M. Zeinoddini, N. Toy & P. Disney (2001) Modelling of tornado and microburst-induced wind loading and failure of a lattice transmission tower. *Engineering structures,* 23**,** 365-375.

Shehata, A., A. El Damatty & E. Savory (2005) Finite element modeling of transmission line under downburst wind loading. *Finite Elements in Analysis and Design* 42**,** 71-89.

Wurman, J. 1998. Preliminary results from the ROTATE-98 tornado study. In *19th Conference on Severe Local Storms*.

Yong, W. & L. Lingyi (2017) One-way Fluid-structure Interaction Analysis of Transmission Tower Under Tornado Loading. *Special Structures***,** 02.

Zhang, Y. (2006) Status quo of wind hazard prevention for transmission lines and countermeasures. *East China Electric Power,* 34**,** 28-31.

Chapter 3

3 Longitudinal reaction on conductors due to tornado wind load

3.1 Introduction

Tornadoes are High Intensity Wind (HIW) events that are formed by an updraft of rising hot air. Those HIW events include downbursts and tornadoes. Both events are characterized by being localized and having a narrow width. Transmission line structures are very long structures as they extend to kilometers. As a result, the probability that a HIW event attacks a portion of a line is quite high. As such, it is important to account for HIW loads in the design of transmission line structures. Historically, over 80% of worldwide transmission line structure failures were deemed to be caused by HIW events (Dempsey and White, 1996). Multiple transmission tower failures caused by tornadoes have been reported in Canada, the United States and China (Narancio et al., 2020, Ekisheva et al., 2021, Zhang, 2006), leading to severe economic loss and negative consequences on residential users. Tornadoes have been rated based on their level of damage by Fujita (1981) and were categories 0 to 5, with 0 being the lowest. This rating was modified to produce the Enhanced Fujita scale, which is used in the United States (McDonald et al., 2010). 86% of tornadoes in the United States can be rated as F2 or lower (ASCE, 2020). A study that considered 1839 tornadoes in Canada reported that most of them (more than 90%) are F2 or less (Hong et al., 2021). Therefore, considering the practicality of designing transmission line structures, the current study mainly focuses on F2 tornadoes.

Because of their localized characteristic and their short-lived duration, the field measurements of tornadoes is very hard. Accordingly, the characterization of the tornado wind load is the first challenge. A linearly distributed tornado wind load acting on the conductors and the tower members was proposed by Ishac and White (1994) for different tornado scales. However, the complicated velocity components of the tornado wind field can not be simplified by linear loading. In order to gain more intuitive full-scale tornado velocity data, Doppler on Wheels (DOW) radars were developed and proved to be reliable field measurement tools (Sarkar et al., 2005). Yet, the data collected by DOW are mainly

from a height of tens of meters above the ground, which can not provide the near-ground data that are most concerned in the structural design. The numerical simulation is another promising option. In order to provide reliable tornado velocity data for structural response numerical analysis, Computational Fluid Dynamic (CFD) simulations were then employed. Some studies simulated the tornado using a two-dimensional axisymmetric model (Rotunno, 1977, Wilson, 1977, Leslie and Smith, 1982, Wilson and Rotunno, 1986), while others simulated the tornado using three-dimensional models (Grasso and Cotton, 1995, Walko, 1990, Sarkar et al., 2005, Xia, 2001). Some attempts for evaluating the tornado forces acting on structures using numerical simulations were also conducted (Panneer Selvam and Millett, 2005, Selvam and Millett, 2003). Later, a CFD model of the F4 tornado, which occurred in Spencer, South Dakota using unsteady Reynolds Averaged Navier-Stokes (RANS) equation was developed by Hangan and Kim (2008). El Damatty et al. (2018) developed CFD simulations of the Stockton tornado that occurred in Kansas, USA, in 2005.

Regarding the response of transmission lines for tornadoes, Savory et al. (2001) conducted a numerical study that focused on the tower without including the conductors. The University of Western Ontario (UWO) conducted an extensive research program to study the behaviour of transmission lines under tornadoes. A major outcome of the research program conducted at the UWO was the development of the load case simulating the critical effect of tornadoes on a generic transmission line structure. Those load cases resulted from the studies conducted by El Damatty and Hamada (2016) and El Damatty et al. (2015) and they were recently incorporated into the American Society of Civil Engineering guideline for transmission lines loading, ASCE-74 (2020). The load cases include defined vertical profiles for the horizontal velocity acting on the tower in two perpendicular directions. In addition, they include an equivalent transverse uniform pressure acting on the conductors. The main objective of this study is to refine those load cases by providing a more accurate estimation for the conductor loads. Because of the localized nature of tornadoes and their complicated three-dimensional wind field, the loads acting on two spans adjacent to a tower will be uneven. This will lead to a net longitudinal force transferred from the conductors to the tower. The estimation of this force is not an easy task for the structural designers as it requires the knowledge of the critical tornado

wind field as well as the critical tornado location maximizing this force. It also requires conducting nonlinear analysis for the conductors taking into account the variation in loading along multi-span of the conductors while accounting for various effects like insulator length and conductor's sag and weight. The calculation of the transverse conductor force is much easier once the pressure distribution is identified. It can be done by summing the pressure from the center of the head to the center of the back span.

The equivalent uniform pressure introduced in the ASCE-74 (2020) is meant to produce the same effect on the tower as the combined effects of the longitudinal and transverse conductor forces. The objective of this Chapter is to develop a set of graphs, which can be easily used to estimate the peak longitudinal force transmitted from the conductors to the tower. Those graphs are developed based on the findings of the previous Chapter, which identified the critical tornado and its critical location, as well the critical conductor heights which should be considered.

The developed set of graphs should account for all the conductor parameters which can affect the value of the longitudinal forces. After the introduction section, the Chapter starts by providing a brief summary of the design load cases recently incorporated in the ASCE-74 (2020). A brief description of the numerical model used in this study together with the applied wind field based on the findings of the previous Chapter, are then presented. A parametric study is then conducted to assess the variation of the longitudinal forces with the parameters that define the structural performance of a conductor. The purpose is to determine the order of variation of the reactions with each parameter.

In view of the results of this parametric study, charts are developed that enable the estimation of the critical longitudinal forces for a generic conductor under the effect of F2 tornadoes. The use of those graphs to estimate the longitudinal force requires adopting a multi-variable line regression, which is provided. A number of conductors are numerically analyzed and the results are used to assess the accuracy of the developed charts. Finally, an example is worked out to illustrate the use of the design charts.

3.2 Numerical model and critical wind field

In the current study, a numerical, analytical technique developed and validated by Aboshosha and El Damatty (2014) is used to conduct the parametric analysis and reaction calculation. This technique accounts for the conductors' nonlinear behaviour, pretension force, sag and the flexibility of the insulators. Figure 3-1 provides the conductor system used in the technique, where L is span length and h is the insulator length. The moment equilibrium is applied on the conductors and insulators, and by solving the equilibrium equation iteratively, the longitudinal force and the reactions are obtained. The main advantage of this technique is the high computational efficiency, which makes massive parametric study possible within a short time period. More details of the technique can be found at Aboshosha and El Damatty (2014).

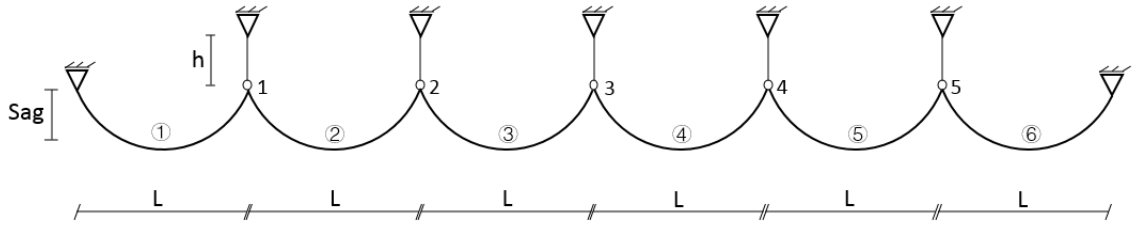

Figure 3-1 Conductor system presented by Aboshosha and El Damatty (2014)

In the previous Chapter, the responses of transmission line conductors under three different tornado wind fields are evaluated and compared. The three tornadoes included are Design Tornado, which is provided by Hamada et al. (2010), Stockton v1 (STV1) tornado and Goshen county v1 (GCV1) tornado which are developed and validated by El Damatty et al.(2018). The critical longitudinal and transverse forces, and their corresponding tornado configurations are estimated. Based on the results of this study, the critical tornado configurations that should be considered for conductor design are: the Design Tornado and STV1 tornado, with H = 50 m, R equals span length, $\theta = 90°$. However, the response of the transmission tower under tornado wind load depends on the reaction generated on conductors as well as the loads acting on the tower itself. Since the tornado configuration for the peak longitudinal reaction is different from the configuration leading to maximum forces acting on the tower, the results corresponding to the peak velocity profile are

extracted and compared. The tornado distance from the tower of interest is determined to be the corresponding radius where maximum tangential velocity occurs. The results reveal that for conductors with a span length smaller than 300 m, the critical tornado is STV1. For conductors with a span length larger than 300m, the critical tornado is Design Tornado. The maximum difference between critical longitudinal reaction caused by STV1 and Design tornado for conductors with small spans is 6%. As such, the Design Tornado is considered in the following study, and the final tornado configuration that is used in this Chapter is: the Design Tornado, with H = 30 m or 35 m, R = 125 m and θ = 15° or 30°.

Figure 3-2 presents the critical tornado location, R and θ, relative to the tower of interest. With the two critical conductor heights (H = 30 m and H = 35 m), four different combinations exist. The envelope of these four combinations is considered. In order to provide a clear insight into the critical configurations, the transverse and axial (vertical) velocity distributions along the span with a span length of 480 m for different configurations are provided in Figure 3-3.

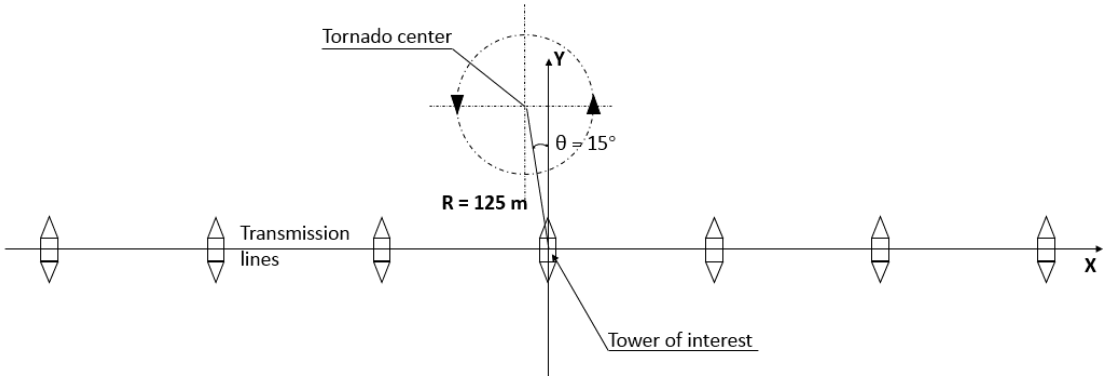

(a)

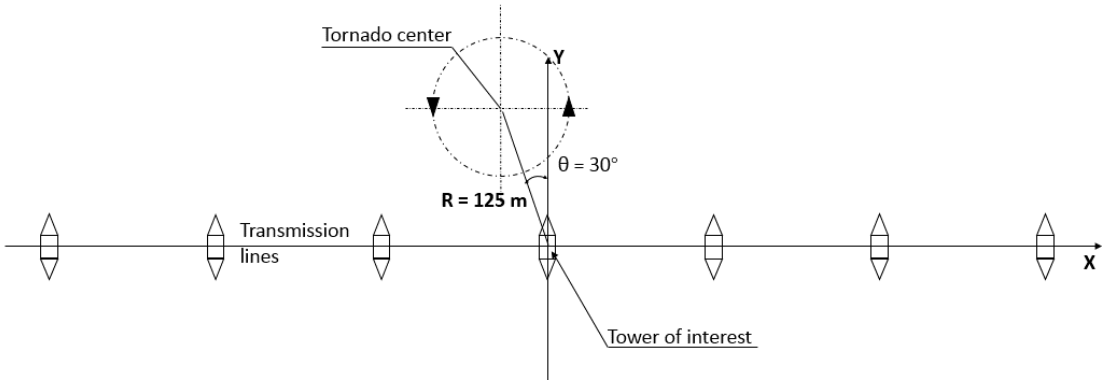

(b)

Figure 3-2 One of the critical tornado configurations, R = 125 m, (a) θ = 15°, (b) 30 °

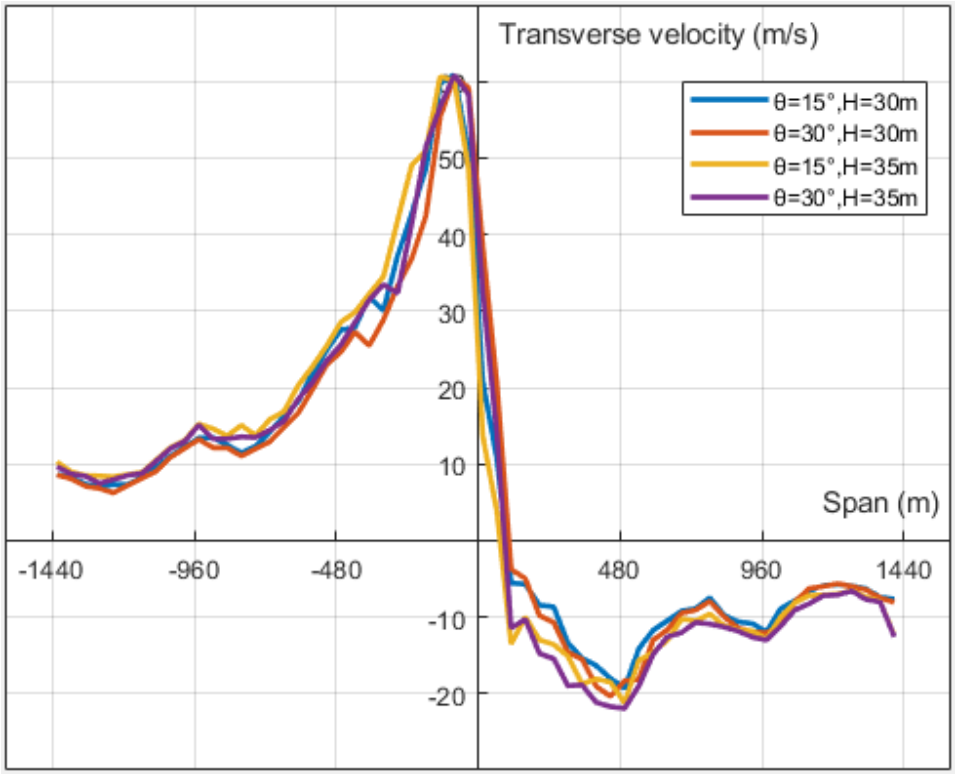

(a)

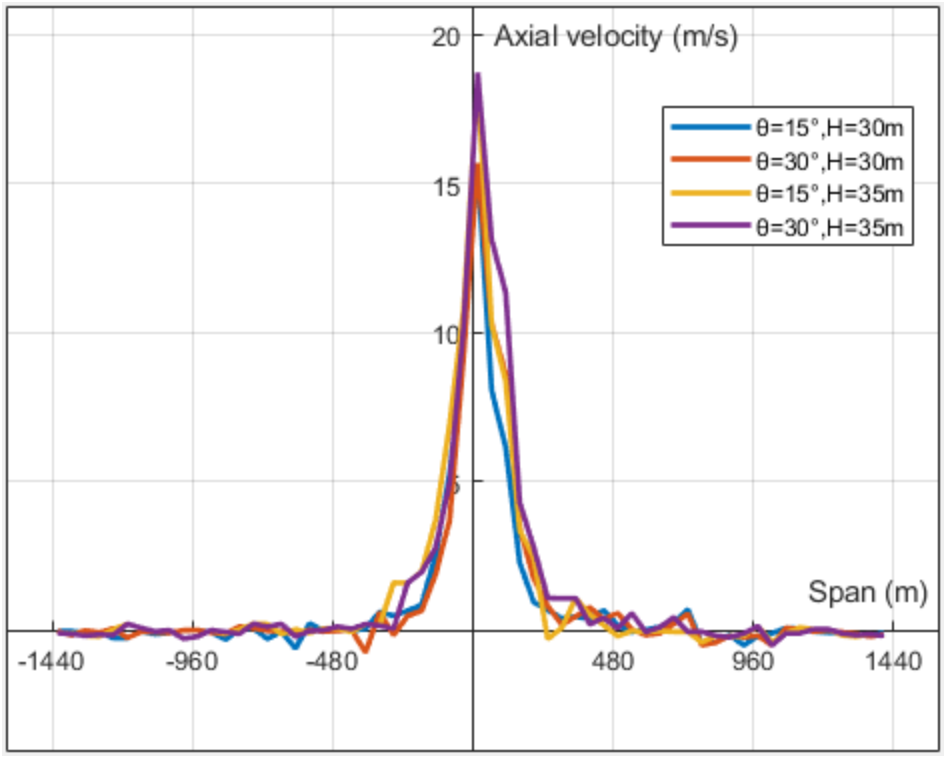

(b)

Figure 3-3 Velocity distribution along conductor spans for critical tornado configurations (a) Tangential velocity (b) Axial velocity

3.3 Parametric study to assess variation of longitudinal force with conductor parameters

Designers need a simple procedure that can be quickly applied to estimate the conductor reactions under the tornado wind load effect. This procedure requires estimating the effect of variation of different conductor parameters on the reaction. Thus, identifying how the various geometric parameters affect the reaction, either linearly or nonlinearly, should be the first step. The considered parameters are a) Young's modulus (E), b) weight per unit length (w), c) projected diameter (d_p), d) sag ratio (S) which is the conductor sag divided by the span (L), e) insulator length (h).

In the above parameters, the d_p is the projected diameter of the conductor in the direction perpendicular to the transverse tornado wind. For each parameter, the practical ranges are determined based on standard conductor parameters obtained from the company Hydro

One Ontario and from other utility companies. Two conductors, cable 1 and cable 2, are considered in this section, whose default values of parameters are provided in Table 3-1.

Table 3-1 Properties of the selected conductors used in the parametric study

Conductor index	Weight per unit length w (N/m)	Projected diameter d_p (m)	Young's modulus E (N/m^2)	Sag ratio S	Span L (m)	Insulator length h (m)	Conductor height (m)	Tornado angle(°)
cable 1	40	0.04	8E+10	4%	200,300,400,500	3	30, 35	15, 30
cable 2	10	0.02	8E+10	2%	200,300,400,500	2	30, 35	15, 30

For each parameter, the study is conducted by following steps:

(1) Develop the conductor model using the semi-analytical technique and employing the default values given in Table 3-1.
(2) One of the parameters (w, d_p, E, S, h) is varied gradually while the other parameters remain with default values.
(3) A tornado angle is assumed (15° or 30°), while the tornado distance is R = 125 m as previously stated.
(4) A conductor height is assumed (30 m or 35 m).
(5) The conductor is analyzed to obtain the longitudinal reaction Rx at the tower of interest.

Steps (1) to (5) are repeated for the four span lengths listed in Table 3-1. For each parameter, the results are presented to show the variation of Rx with this specific parameter:

1. Effect of weight per unit length w

Figures 3-4 and 3-5 show that reaction Rx decreases nonlinearly with increasing the conductor's weight per unit length. As w increases, the conductor's stiffness will also increase due to the corresponding rising pretension force, which reduces the longitudinal

force. The effect of w to Rx can be classified as linear within two ranges, 10 N/m ≤ w ≤ 25 N/m and 25 N/m ≤ w ≤ 40 N/m.

2. Effect of projected diameter d_p

Figures 3-6 and 3-7 presents the effect of d_p on Rx, showing nonlinear behaviour for the heavy conductor. The longitudinal force increases when d_p increases. Thus, the relationship between d_p and Rx can be considered linear within two separated regions, 0.02 m ≤ d_p ≤ 0.044m and 0.044 m ≤ d_p ≤ 0.08m.

3. Effect of conductor's sag ratio S

The sag ratio S is defined as line sag divided by conductor span length L. The considered range of S varies from 2% to 4%, with an increment of 0.5%. Figures 3-8 and 3-9 show that for both conductors cable 1 and cable 2, a larger sag ratio S leads to a larger reaction. This is reasonable since the increase in S will cause a reduction in pretension force, therefore leading to the decline in conductor stiffness. The corresponding longitudinal reaction Rx will increase as a result. The relationship between Rx and S is almost linear.

4. Effect of insulator length h

The range of insulator length h varies from 1m to 5m, with an increment of 1m. Figures 3-10 and 3-11 show that the longitudinal reaction R_x changes nonlinearly with h. The increase in h results in a reduction in R_x, as explained by Aboshosha and Damatty (2014).

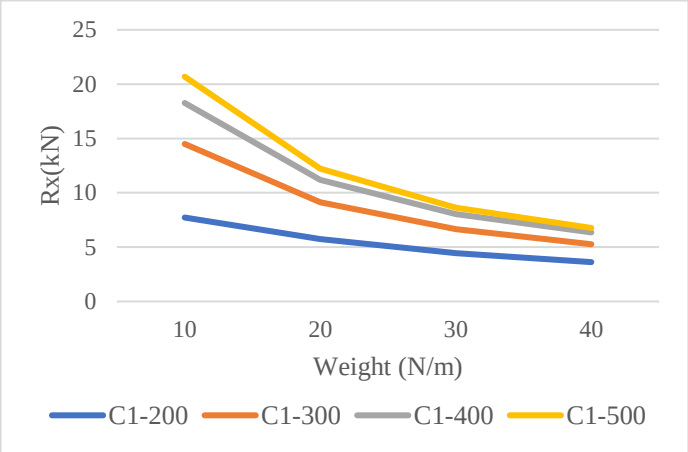

Figure 3-4 Variation of Rx with w for C1

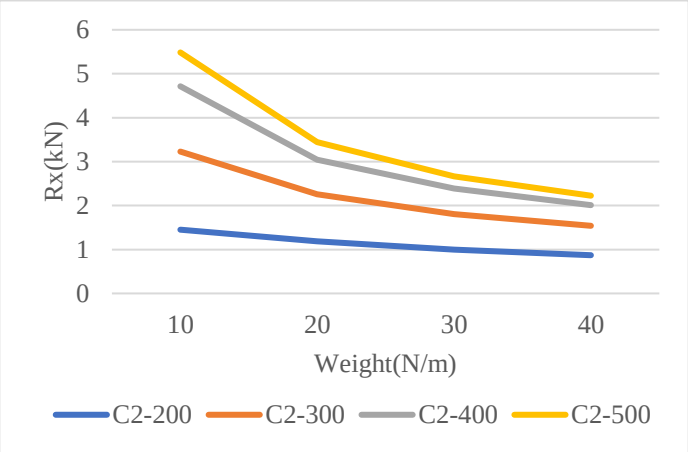

Figure 3-5 Variation of Rx with w for C2

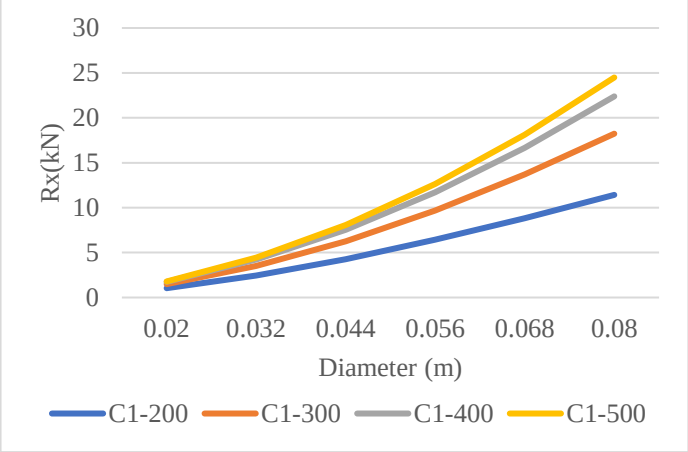

Figure 3-6 Variation of Rx with dp for C1

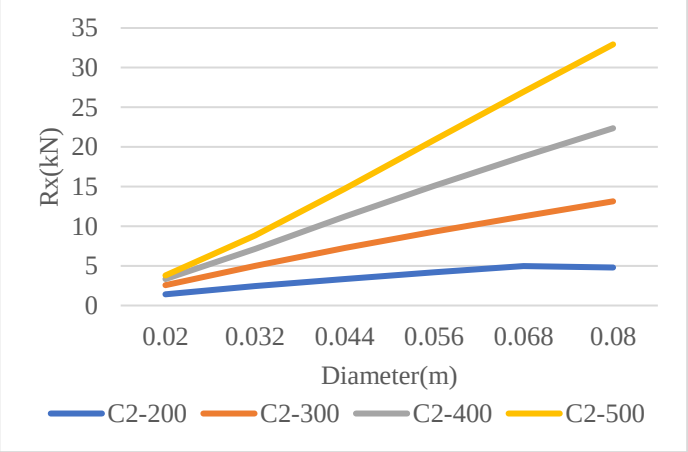

Figure 3-7 Variation of Rx with dp for C2

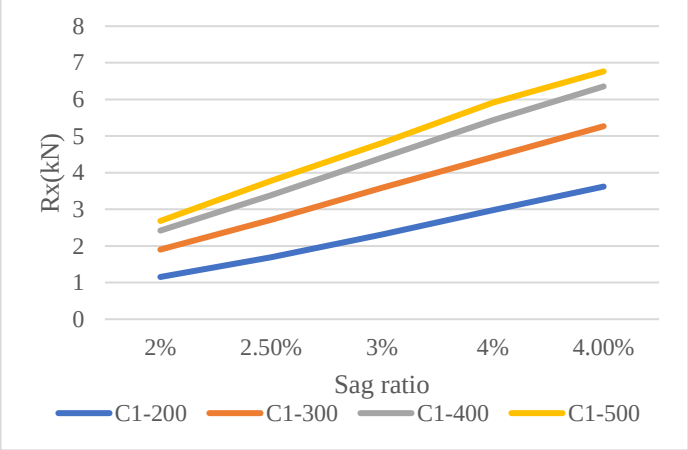

Figure 3-8 Variation of Rx with S for C1

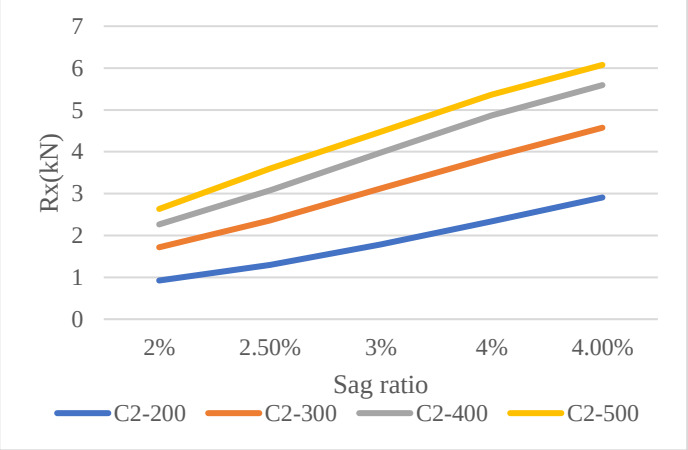

Figure 3-9 Variation of Rx with S for C2

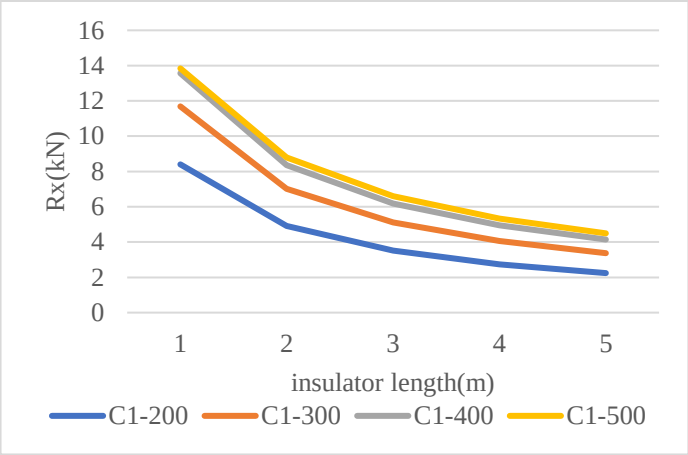

Figure 3-10 Variation of Rx with h for C1

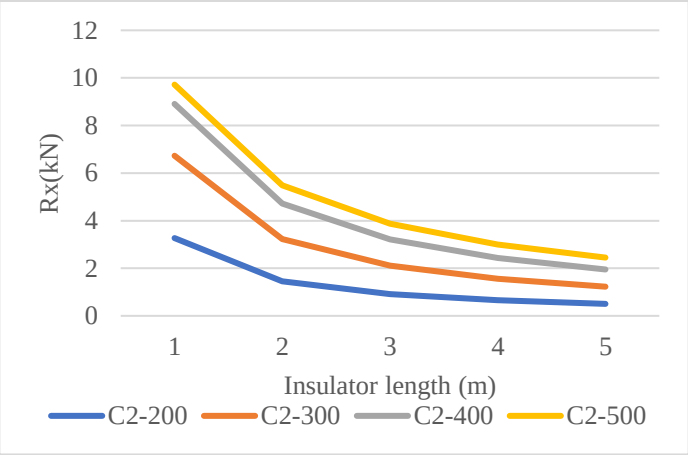

Figure 3-11 Variation of Rx with h for C2

5. Effect of Young's modulus E.

Young's modulus varies from 6E+10 N/m^2 to 8E+10 N/m^2. The variation of Young's modulus has a negligible effect on the longitudinal reaction.

The conclusion of the parametric study is presented in Table 3-2.

Table 3-2 The effect of each parameter on Rx

Conductor parameter	The effect on R_x
Weight per unit length w	Varies linearly within two ranges: 10 N/m ≤ w ≤ 25 N/m and 25 N/m ≤ w ≤ 40 N/m
Projected diameter d_p	Varies linearly within two ranges: 0.02 m ≤ d_p ≤ 0.044 m and 0.044 m ≤ d_p ≤ 0.08 m
Sag ratio S	Varies linearly with S
Insulator length h	Varies nonlinearly with h
Young's modulus E	Negligible effect

3.4 Longitudinal force charts under tornado wind load

In order to estimate the longitudinal reaction Rx of conductors with different parameters under critical tornado wind load described in the previous section, a set of charts are developed and provided in Appendix I. In order to obtain the critical reaction, the charts are taken as the envelope of reactions calculated with four different combinations of tornado position and conductor height. The charts are only applicable to tangent towers where the towers are linearly aligned and the conductors are connected to the towers through insulators. The longitudinal reactions on ground wires can not be calculated using the current method.

Based on the previous parametric study that identified each parameter's effect on the longitudinal reaction, the charts can cover a practical range of conductor parameters w, d_p, S, h and L. The charts are developed based on the following findings:

a) For the considered range of S, the longitudinal reaction Rx varies linearly.
b) Rx varies nonlinearly with w and d_p. However, if the domains of each parameter (10 N/m $\leq$ w $\leq$ 40 N/m and 0.02 m $\leq$ d_p $\leq$ 0.08 m) are divided into two regions, the variation of R_x with w and d_p can be considered linear within each region.
c) The effects of L and h on R_x are nonlinear. As such, charts are developed to show the variation of R_x with L for different values of h.

Combining all the above findings, four groups of charts are developed depending on the upper and lower limit of w and d_p. The range of different groups is provided in Table 3-3. In order to cover all possible combinations of w_{min}, w_{max}, d_{pmin}, d_{pmax}, eight charts are provided for each group with the corresponding range of w and d_p, S_{min} = 2% and S_{max} = 4%.

Conductor reaction R_x changes linearly within each group with w, d_p and S. Therefore, the corresponding value of R_x with specific d_p, w, S, h and L within the range can be calculated using a three-dimensional linear interpolation.

Table 3-3 The range of parameters within different groups

Group	d_p (m)		w (N/m)		S(%)	
	d_{pmin}	d_{pmax}	w_{min}	w_{max}	S_{min}	S_{max}
Ⅰ	0.02	0.044	10	25	2	4
Ⅱ	0.02	0.044	25	40	2	4
Ⅲ	0.044	0.08	10	25	2	4
Ⅳ	0.044	0.08	25	40	2	4

The following steps present the process of evaluating the maximum longitudinal reaction R_x of a conductor subjected to critical F2 tornado load.

1. Based on the conductor's weight per unit length w and the conductor projected diameter d_p, select the corresponding group from Ⅰ to Ⅳ.
2. Based on the conductor span and sag ratio, the user can calculate eight longitudinal reactions using the eight graphs of the selected group, which are given in Appendix I as shown below:

   R_{X1}= force corresponding to (d_{pmin}, w_{min}, S_{min})

   R_{X2}= force corresponding to (d_{pmax}, w_{min}, S_{min})

   R_{X3}= force corresponding to (d_{pmin}, w_{max}, S_{min})

   R_{X4}= force corresponding to (d_{pmax}, w_{max}, S_{min})

   R_{X5}= force corresponding to (d_{pmin}, w_{min}, S_{max})

   R_{X6}= force corresponding to (d_{pmax}, w_{min}, S_{max})

   R_{X7}= force corresponding to (d_{pmin}, w_{max}, S_{max})

   R_{X8}= force corresponding to (d_{pmax}, w_{max}, S_{max})

Where S_{min} = 2% and S_{max} = 4%, d_{pmax} and w_{max} are the upper limits of the conductor's projected diameter and the conductor's weight per unit length for the selected group, and d_{pmin} and w_{min} are the lower limits of the conductor's projected diameter and the conductor's weight per unit length for the selected group.

3. Based on the linearity relationship between parameters d_p, w and S with respect to R_x, linear interpolation can be conducted using equations presented below:

$$R_{x(1-2)} = R_{x1} + (R_{x2} - R_{x1}) * \frac{(d_p - d_{pmin})}{(d_{pmax} - d_{pmin})}$$

$$R_{x(3-4)} = R_{x3} + (R_{x4} - R_{x3}) * \frac{(d_p - d_{pmin})}{(d_{pmax} - d_{pmin})}$$

$$R_{x(Smin)} = R_{x(3-4)} + \left(R_{x(1-2)} - R_{x(3-4)}\right) * \frac{(w_{max} - w)}{(w_{max} - w_{min})}$$

$$R_{x(5-6)} = R_{x5} + (R_{x6} - R_{x5}) * \frac{(d_p - d_{pmin})}{(d_{pmax} - d_{pmin})}$$

$$R_{x(7-8)} = R_{x7} + (R_{x8} - R_{x7}) * \frac{(d_p - d_{pmin})}{(d_{pmax} - d_{pmin})}$$

$$R_{x(Smax)} = R_{x(7-8)} + \left(R_{x(5-6)} - R_{x(7-8)}\right) * \frac{(w_{max} - w)}{(w_{max} - w_{min})}$$

$$R_x = R_{x(Smax)} + \frac{\left(R_{x(Smin)} - R_{x(Smax)}\right)}{(S_{max} - S_{min})} * (S_{max} - S)$$

where d_p, w and S are the actual conductor parameters, d_{pmax} and d_{pmin} are the selected group's upper and lower limits of the conductor projected diameter, respectively, and w_{max} and w_{min} are the selected group's upper and lower limits of the weight per unit length, respectively. Figure 3-13 shows a flow chart that summarizes the previous steps.

Full illustrated charts for Group 1 0.02 m ≤ d_p ≤ 0.044 m & 10 N/m ≤ w ≤ 25 N/m are presented in Figure 3-12. The rest charts are provided in Appendix, I.

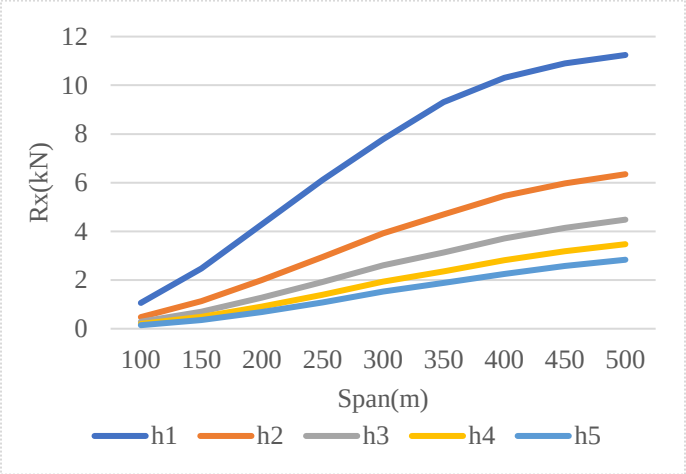

d_{pmin} = 0.02 m, w_{min} = 10N/m, S_{min} = 2%

R_{x1}

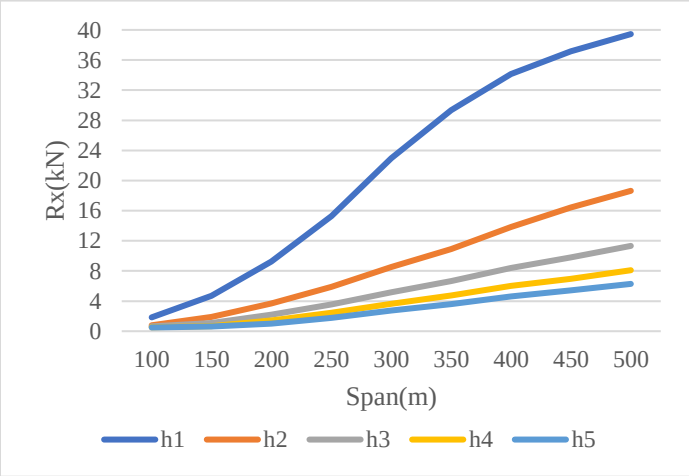

d_{pmax} = 0.044 m, w_{min} = 10N/m, S_{min} = 2%

R_{x2}

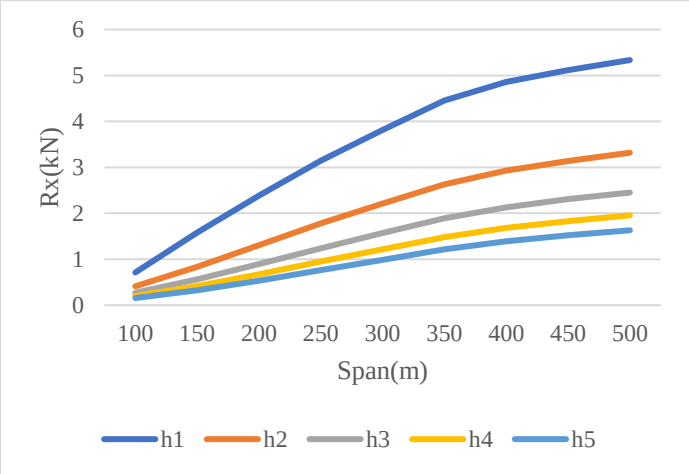

d_{pmin} = 0.02 m, w_{max} = 25 N/m, S_{min} = 2%

R_{x3}

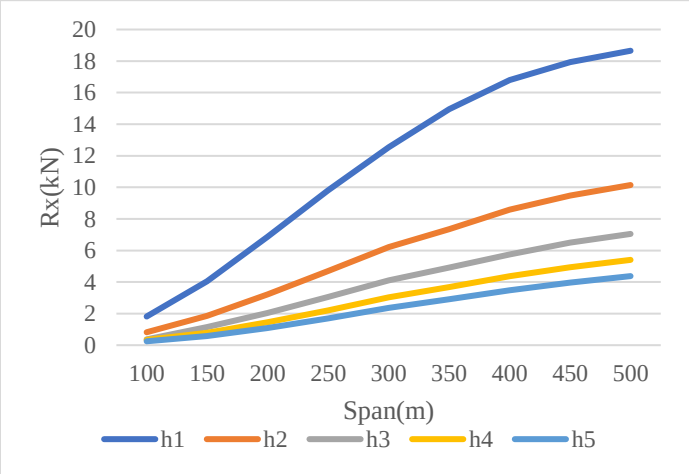

dp_{max} = 0.044 m, w_{max} = 25 N/m, S_{min} = 2%

R_{x4}

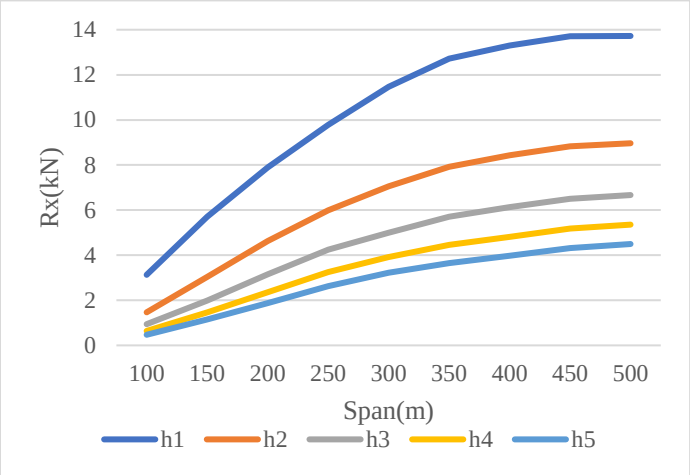

d_{pmin} = 0.02 m, w_{min} = 10N/m, S_{max} = 4%

R_{x5}

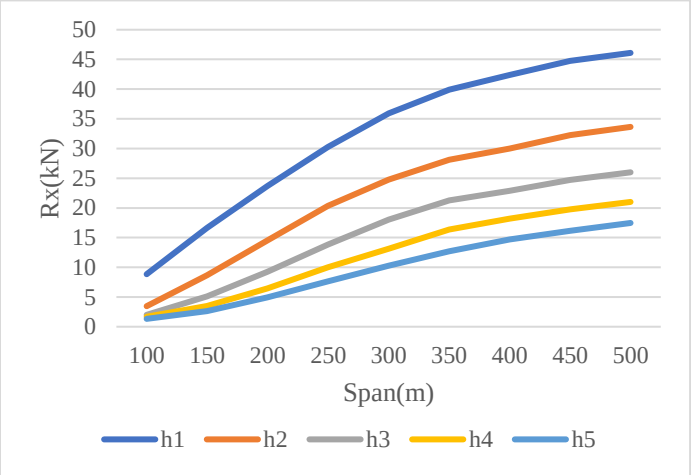

d_{pmin} = 0.044 m, w_{min} = 10N/m, S_{max} = 4%

R_{x6}

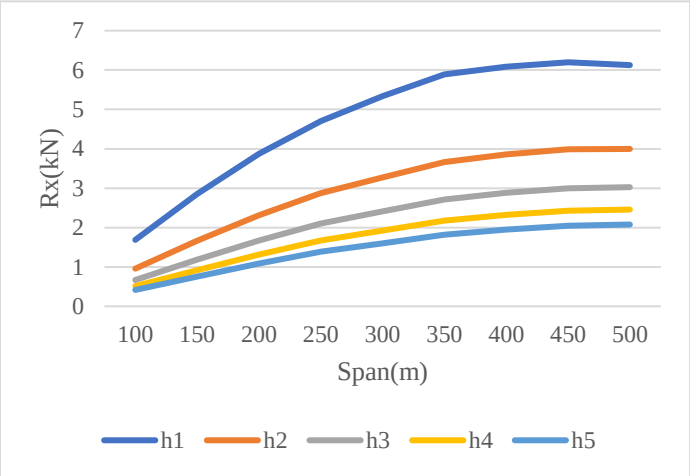

d_{pmin} = 0.02 m, w_{max} = 25N/m, S_{max} = 4%

R_{x7}

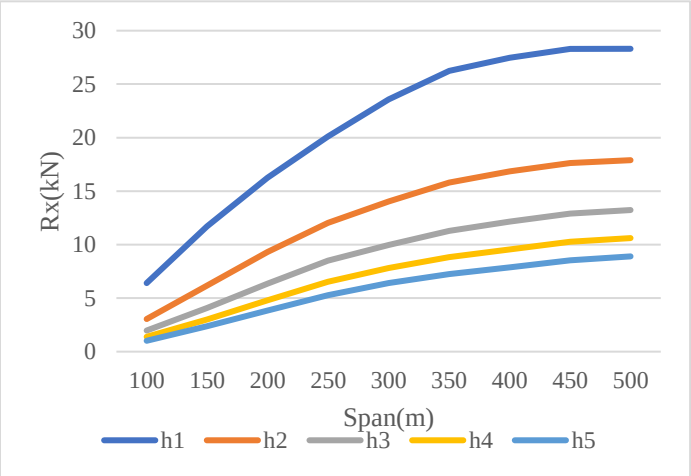

d_{pmax} = 0.044 m, w_{max} = 25N/m, S_{max} = 4%

R_{x8}

Figure 3-12 The charts for Group 1 0.02 m ≤ d_p ≤ 0.044 m & 10 N/m ≤ w ≤ 25 N/m

It is important to note that the tornado wind speeds considered in the current procedure are scaled up to the maximum 3s-gust velocity of F2 tornadoes, where the turbulence is included. Therefore, both the fluctuating component and the mean responses are considered in the current procedure of evaluating longitudinal reaction R_x. Due to the non-correlation of turbulence along the spans, the tornado loading can be reduced by a span reduction factor. However, according to Madugula et al. (2001), the tornado processes turbulence less in magnitude than a regular wind event. Therefore, the span reduction factor is close

to 1 as recommended in the previous study. The large aerodynamic damping of the conductors makes it reasonable to neglect the resonant response. Hamada and El Damatty (2015) also studied the dynamic response caused by the tornado. They concluded that no dynamic effect needed to be considered due to the large aerodynamic damping of the conductors.

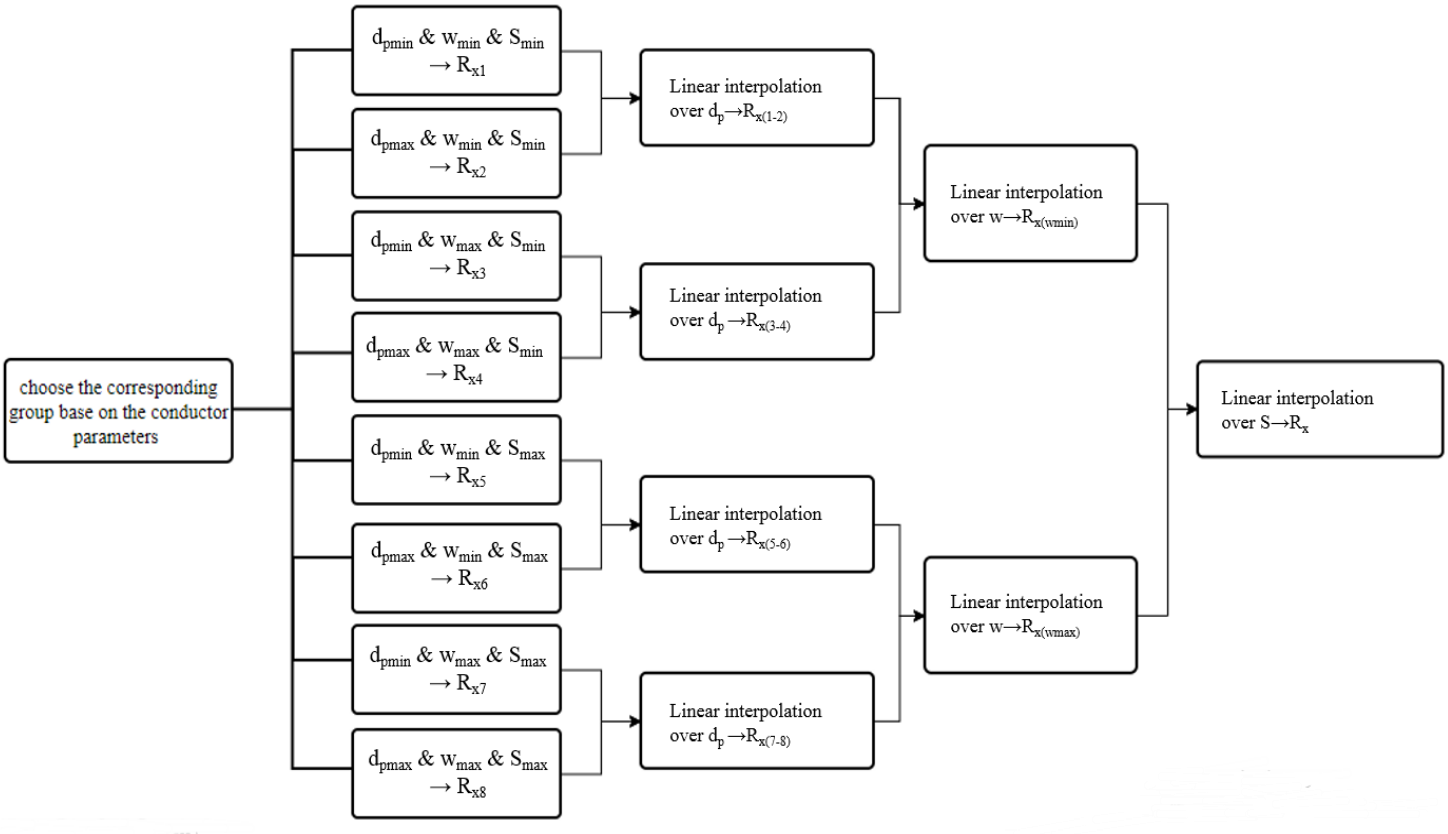

Figure 3-13 Flow charts of the interpolation process to obtain the conductor critical longitudinal force under tornado wind loading

3.5 Validation

The validation of the interpolation procedure is conducted by comparing the longitudinal reaction $R_{x,graph}$ obtained from the graphs to $R_{x,numerical}$ calculated using numerical method. When calculating $R_{x,numerical}$, four different combinations of critical tornado position and conductor height are considered (H = 30 m or 35 m, θ = 15° or 30°). The presenting reaction is the envelope results of the four combinations. The results and corresponding conductor parameters are presented in Table 3-4. Multiple different combinations are considered to

cover all four chart groups. According to the table, $R_{x,numerical}$ are mostly smaller than $R_{x,graph}$, which indicates that the current procedure generates more conservative results than the actual reactions.

Table 3-4 The validations for Rx and the corresponding differences

Span (m)	Sag (m)	sag ratio	Diameter (m)	Weight (N/m)	insulator length(m)	$R_{x,graph}$ (kN)	$R_{x,numerical}$ (kN)	Difference (%)
180	4	2.22%	0.03	15	2.44	2.14	1.87	12.38
250	7	2.80%	0.05	20	3	7.22	6.52	9.77
320	10	3.13%	0.02	20	4	2.25	2.07	7.71
460	18	3.91%	0.06	40	4.27	12.26	11.63	5.13
400	12	3.00%	0.05	30	1.5	19.78	17.84	9.79
450	18	4.00%	0.02	35	3.3	2.22	2.23	-0.64

3.6 Example

An example of using the proposed charts to obtain the longitudinal reaction of the conductor under a tornado is provided in this section to demonstrate the solution steps.

Design Data

Wind span =400 m

Length of insulator assembly = 1.5 m.

Conductor weight per unit length = 30 N/m

Conductor projected diameter= 0.05 m

Line sag= 12 m (~3.00% span)

Based on the provided data, the following classification can be made:

$d_p = 0.05$ m → $0.044 \leq d_p \leq 0.08$ & w = 30 N/m → $25 \leq w \leq 40$ → Group 4

According to the charts corresponding to Group 4, the following values can be calculated:

Rx1 = 12 kN Rx2 = 33 kN

Rx3 = 9 kN Rx4 = 23kN

Rx5 = 22 kN Rx6 = 59 kN

Rx7 = 15 kN Rx8 = 45 kN

The following calculations can be conducted:

$$R_{X(1-2)} = R_{X1} + (R_{X2} - R_{X1}) * \frac{(d_p - d_{pmin})}{(d_{pmax} - d_{pmin})}$$

$$R_{X(1-2)} = 12 + (33 - 12) * \frac{(0.05 - 0.044)}{(0.08 - 0.044)} = 15.5\text{kN}$$

$$R_{x(3-4)} = R_{x3} + (R_{x4} - R_{x3}) * \frac{(d_p - d_{pmin})}{(d_{pmax} - d_{pmin})}$$

$$R_{x(3-4)} = 9 + (23 - 9) * \frac{(0.05 - 0.044)}{(0.08 - 0.044)} = 11.33 \text{ kN}$$

$$R_{x(Smin)} = R_{x(3-4)} + \left(R_{x(1-2)} - R_{x(3-4)}\right) * \frac{(w_{max} - w)}{(w_{max} - w_{min})}$$

$$R_{x(Smin)} = 11.33 + (15.5 - 11.33) * \frac{(40 - 30)}{(40 - 25)} = 14.11 \text{ kN}$$

$$R_{x(5-6)} = R_{x5} + (R_{x6} - R_{x5}) * \frac{(d_p - d_{pmin})}{(d_{pmax} - d_{pmin})}$$

$$R_{X(5-6)} = 22 + (59 - 22) * \frac{(0.05 - 0.044)}{(0.08 - 0.044)} = 28.17 \text{ kN}$$

$$R_{x(7-8)} = R_{x7} + (R_{x8} - R_{x7}) * \frac{(d_p - d_{pmin})}{(d_{pmax} - d_{pmin})}$$

$$R_{X(7-8)} = 15 + (45 - 15) * \frac{(0.05 - 0.044)}{(0.08 - 0.044)} = 20 \text{ kN}$$

$$R_{x(Smax)} = R_{x(7-8)} + \left(R_{x(5-6)} - R_{x(7-8)}\right) * \frac{(w_{max} - w)}{(w_{max} - w_{min})}$$

$$R_{x(Smax)} = 20 + (28.17 - 20) * \frac{(40 - 30)}{(40 - 25)} = 25.45 \text{ kN}$$

The final longitudinal reaction can be calculated:

$$R_x = R_{x(Smax)} + \frac{\left(R_{x(Smin)} - R_{x(Smax)}\right)}{(S_{max} - S_{min})} * (S_{max} - S)$$

$$R_x = 25.45 + \frac{(14.11 - 25.45)}{(4 - 2)} * (4 - 3) = 19.78 \text{ kN}$$

3.7 Conclusion

In this Chapter, a simplified procedure is proposed to allow a quick estimate of the critical longitudinal force transmitted from the conductor to a tower under tornado wind loads. Based on the finding of the previous Chapter regarding the critical tornado position relative to the transmission line structure system, two different tornado angles and two different conductor heights are considered, and the envelope of different combinations is taken in

the following study when calculating the longitudinal reactions. At this critical tornado position, a parametric study is conducted to evaluate the effect of different conductor parameters on the longitudinal response. The following conclusions can be drawn from the study related to the variation of longitudinal reaction R_x with the conductor parameters:

a) Rx decreases nonlinearly as the conductor weight w increases. However, if dividing the range of w into two regions, R_x changes linearly within each region.
b) Rx increases nonlinearly as the conductor projected area d_p increases. If the range of d_p is divided into two regions, R_x can also be considered changing linearly within each region.
c) Rx changes linearly with the sag ratio S.
d) Rx changes nonlinearly with insulator length h.
e) There is no obvious effect of Young's Modulus E on R_x.

Rx varies linearly if the practical range of w and d_p is divided into two different regions separately. Therefore, the entire domain for w and d_p can be divided into four regions, where within each region R_x varies linearly with w, d_p and S. For each region, the variations of R_x with the conductor span L, and the insulator length h, are provided for the combinations of the upper and lower values of w, d_p and S corresponding to each region. The force R_x can be then estimated by applying a three-dimensional linear interpolation using the values corresponding to the upper and lower limits of w, d_p and S. A validation of the proposed approach is conducted by comparing the values estimated using the developed graphs and the interpolation procedure to those obtained from numerical analysis. Finally, an example is provided to illustrate the steps involved in the proposed approach.

3.8 Acknowledgment

The authors would like to acknowledge Hydro One Ontario Company Canada and the Natural Sciences and Engineering Research Council of Canada (NSERC) for their in-kind support, their collaboration in this project, and for the financial support provided for this research.

3.9 Appendix I

Group 2 0.02 m ⩽ d_p ⩽ 0.044 m & 25 N/m ⩽ w ⩽ 40 N/m

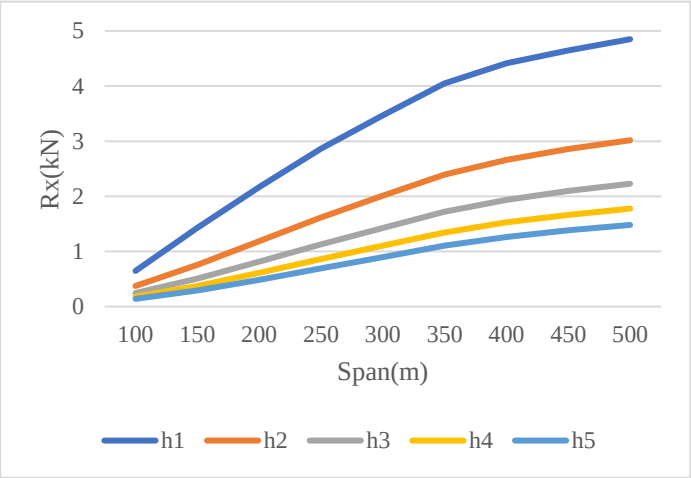

d_{pmin} = 0.02 m, w_{min} = 25N/m, S_{min} = 2%

R_{x1}

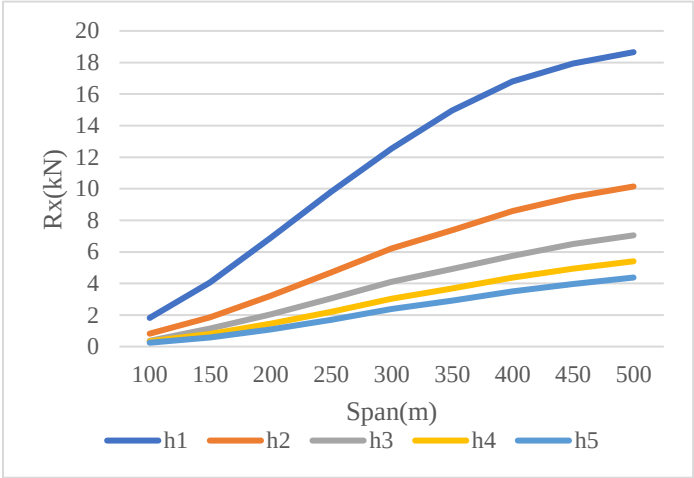

d_{pmax} = 0.044 m, w_{min} = 25N/m, S_{max} = 2%

R_{x2}

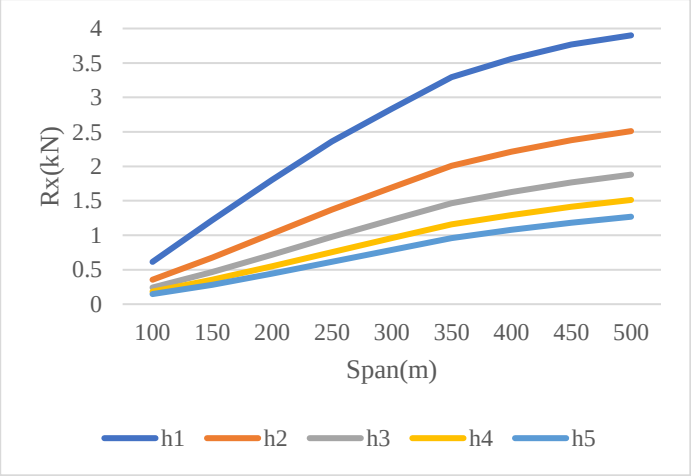

d_{pmax} = 0.02 m, w_{max} = 40N/m, S_{min} = 2%

R_{x3}

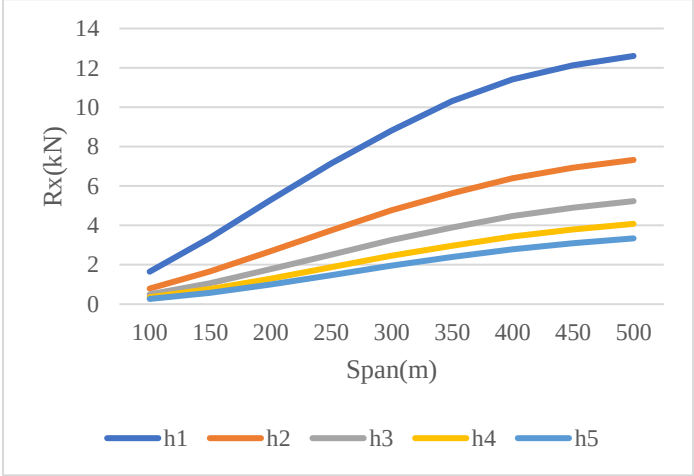

d_{pmax} = 0.044 m, w_{max} = 40N/m, S_{max} = 2%

R_{x4}

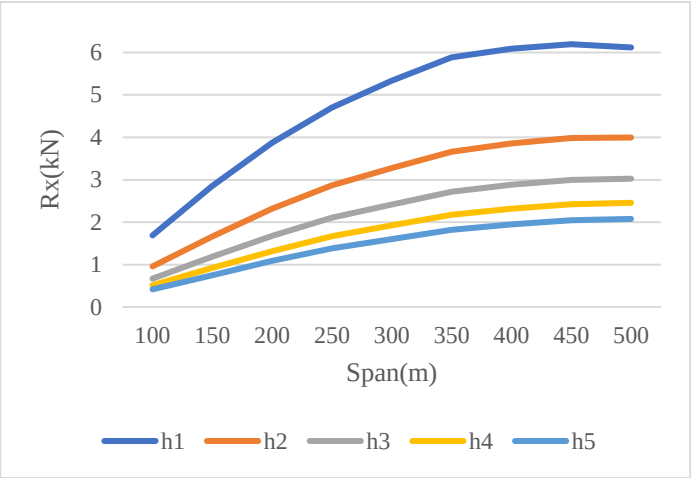

d_{pmin} = 0.02 m, w_{min} = 25N/m, S_{min} = 4%

R_{x5}

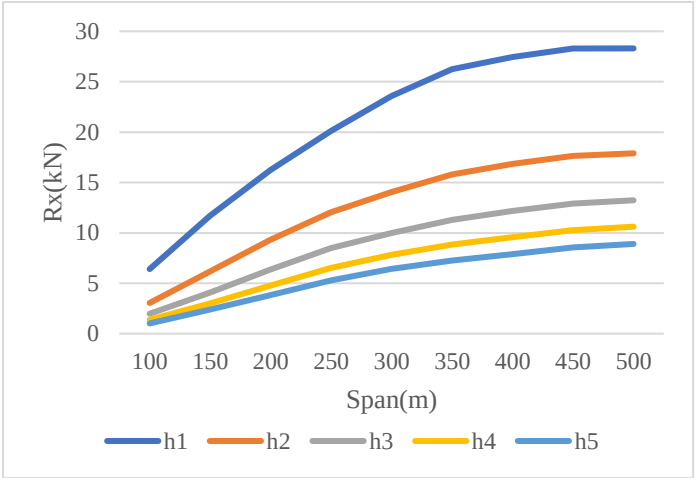

d_{pmax} = 0.044 m, w_{min} = 25N/m, S_{max} = 4%

R_{x6}

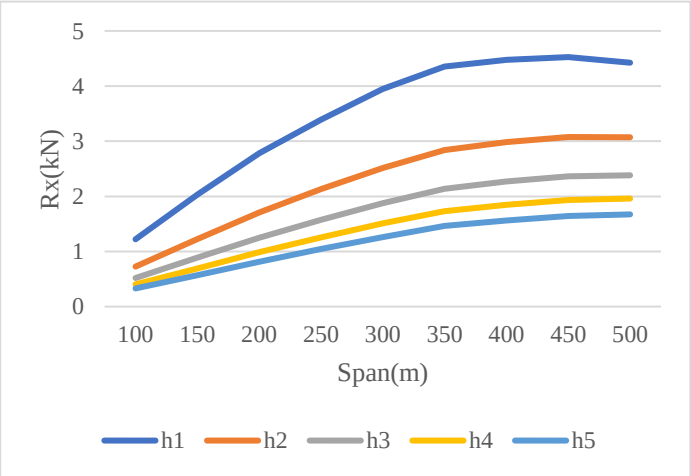

d_{pmin} = 0.02 m, w_{max} = 40N/m, S_{max} = 4%

R_{x7}

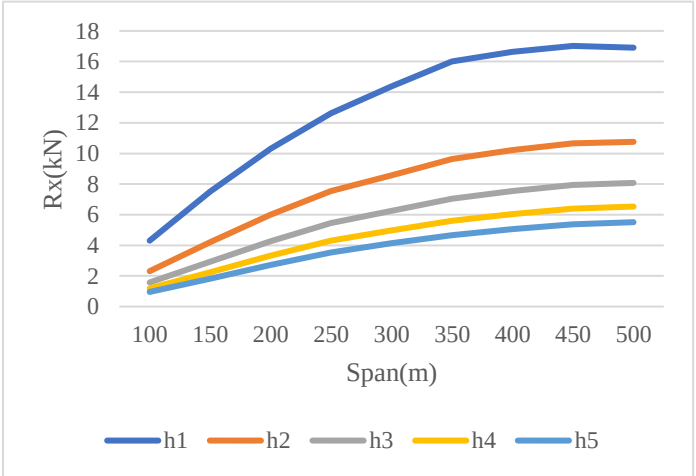

d_{pmax} = 0.044 m, w_{max} = 40N/m, S_{max} = 4%

R_{x8}

Group 3 0.044 m ⩽ d_p ⩽ 0.08 m & 10 N/m ⩽ w ⩽ 25 N/m

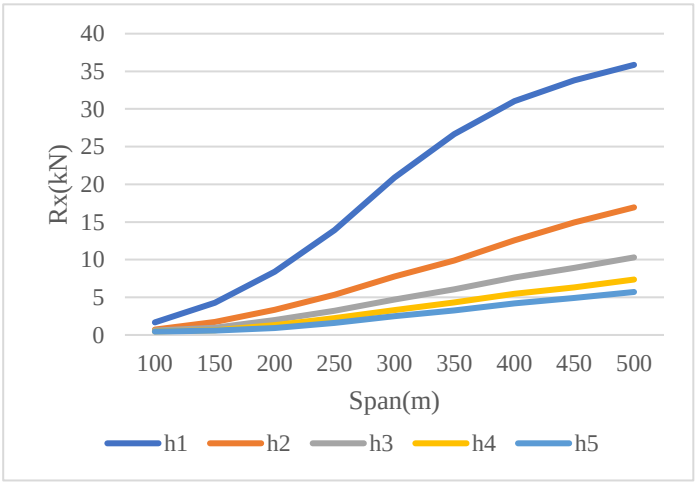

d_{pmin} = 0.044 m, w_{min} = 10N/m, S_{min} = 2%

R_{x1}

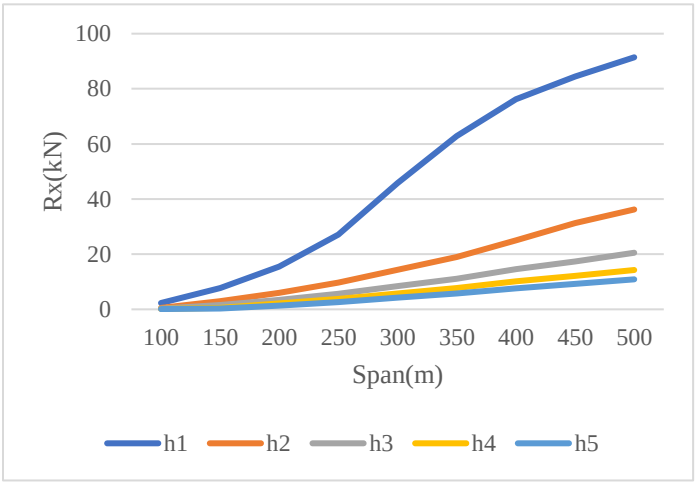

d_{pmax} = 0.08 m, w_{min} = 10N/m, S_{min} = 2%

R_{x2}

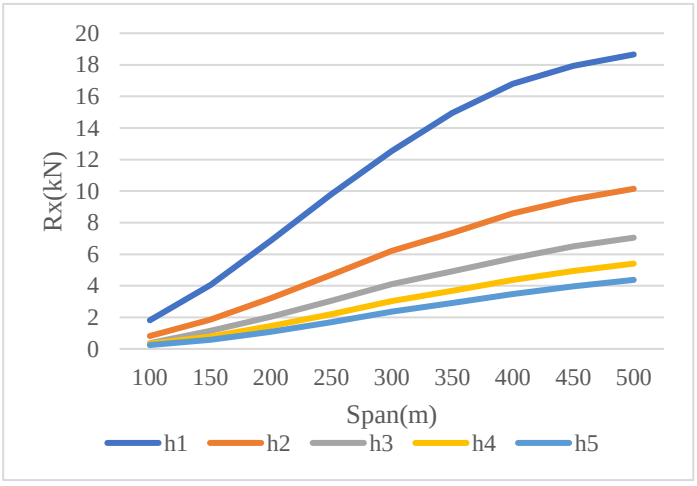

d_{pmin} = 0.044 m, w_{max} = 25N/m, S_{min} = 2%

R_{x3}

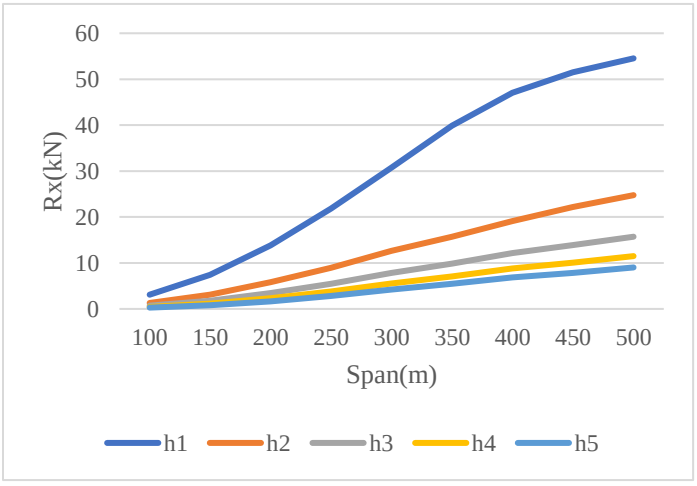

d_{pmax} = 0.08 m, w_{max} = 25N/m, S_{min} = 2%

R_{x4}

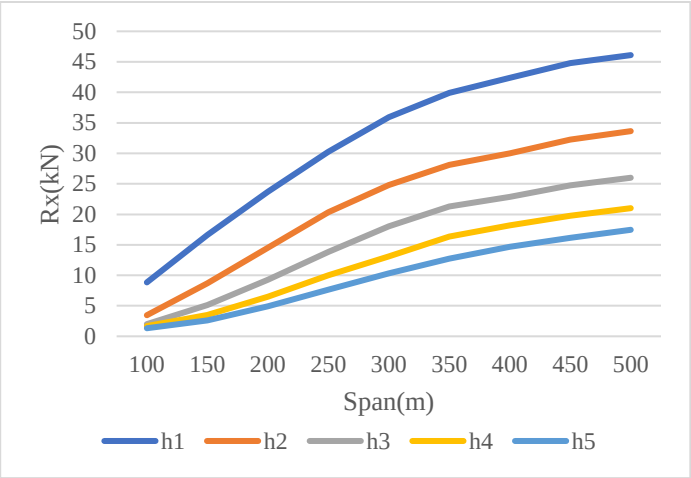

d_{pmin} = 0.044 m, w_{min} = 10N/m, S_{max} = 4%

R_{x5}

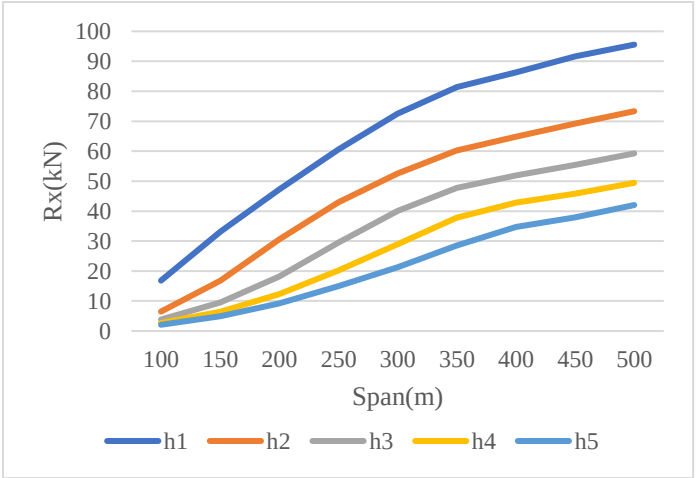

d_{pmax} = 0.08 m, w_{min} = 10N/m, S_{max} = 4%

R_{x6}

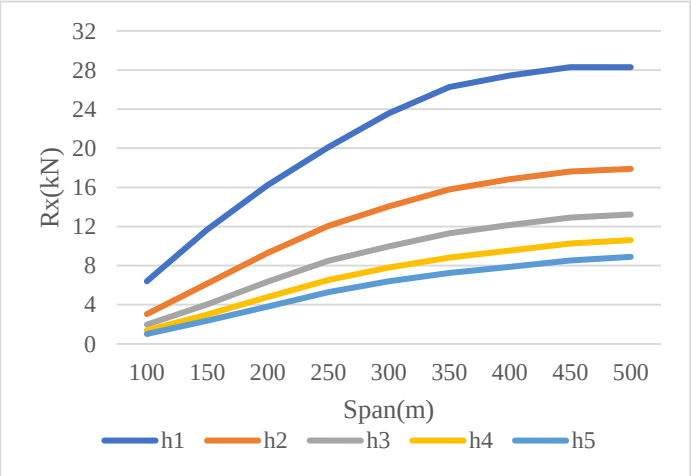

d_{pmin} = 0.044 m, w_{max} = 25N/m, S_{max} = 4%

R_{x7}

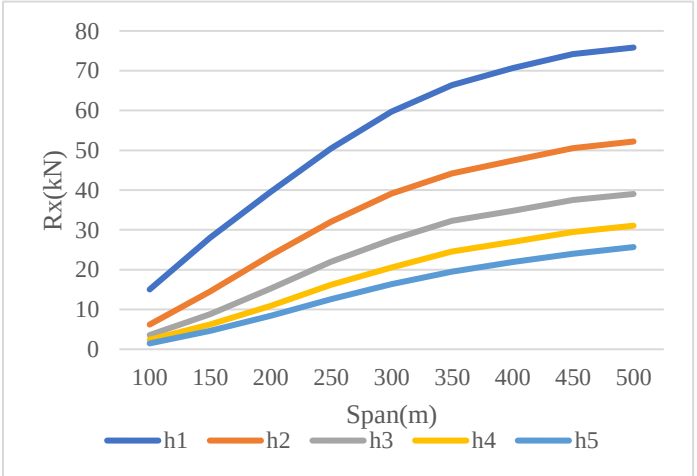

d_{pmax} = 0.08 m, w_{max} = 25N/m, S_{max} = 4%

R_{x8}

Group 4 0.044 m ⩽ d_p ⩽ 0.08 m & 25 N/m ⩽ w ⩽ 40 N/m

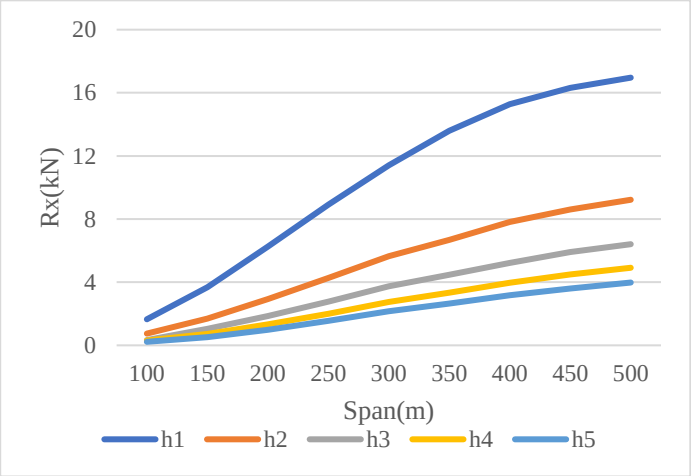

d_{pmin} = 0.044 m, w_{min} = 25N/m, S_{min} = 2%

R_{x1}

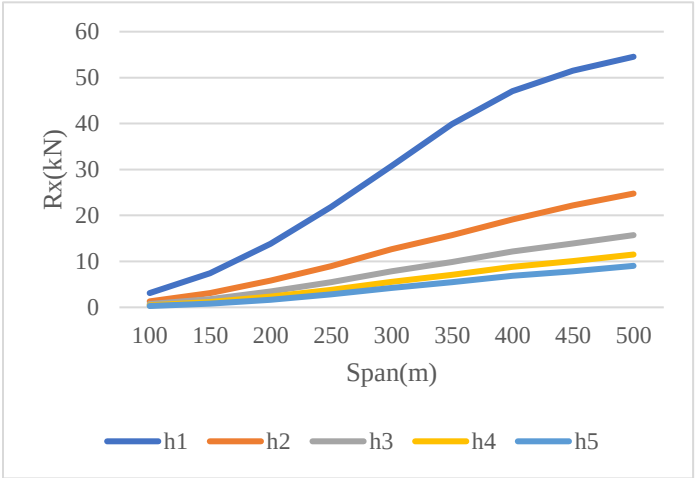

d_{pmax} = 0.08 m, w_{min} = 25N/m, S_{min} = 2%

R_{x2}

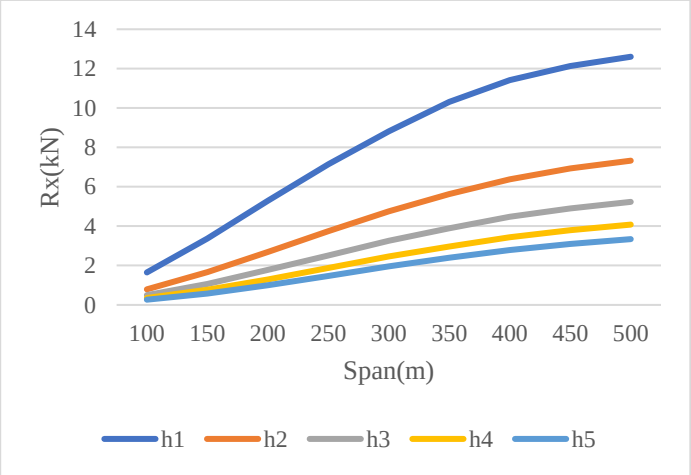

d_{pmin} = 0.044 m, w_{max} = 40N/m, S_{min} = 2%

R_{x3}

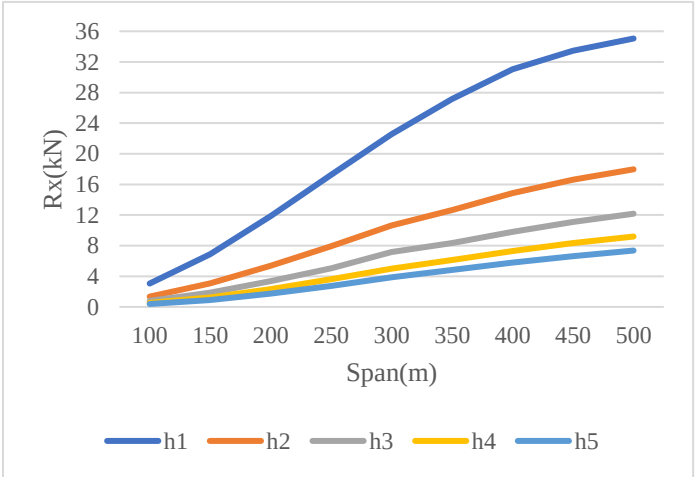

d_{pmax} = 0.08 m, w_{max} = 40N/m, S_{min} = 2%

R_{x4}

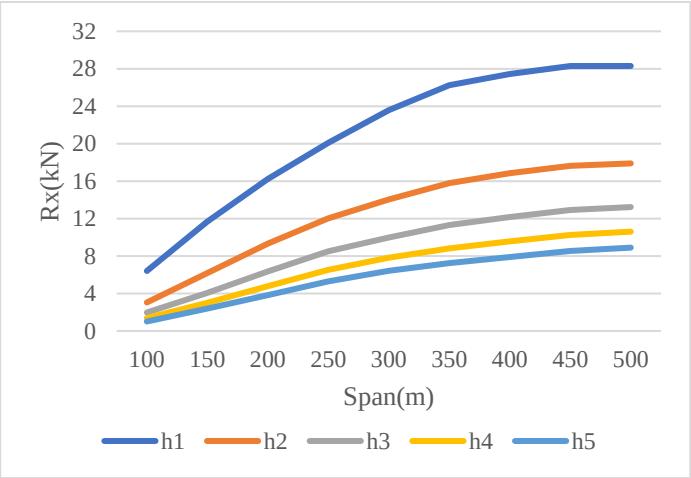

d_{pmin} = 0.044 m, w_{min} = 25N/m, S_{max} = 4%

R_{x5}

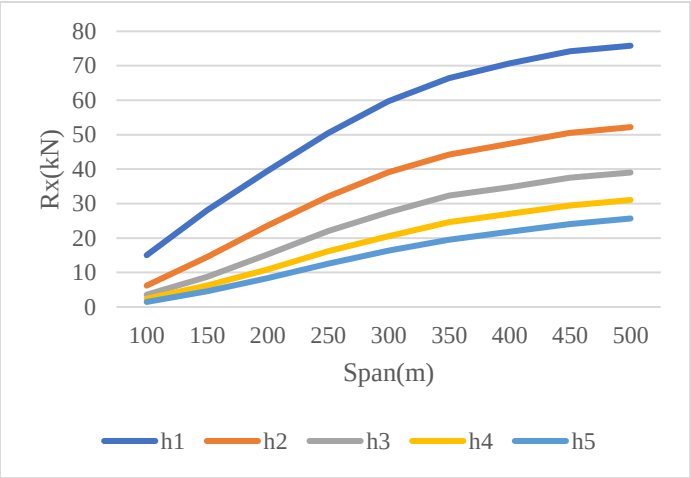

d_{pmax} = 0.08 m, w_{min} = 25N/m, S_{max} = 4%

R_{x6}

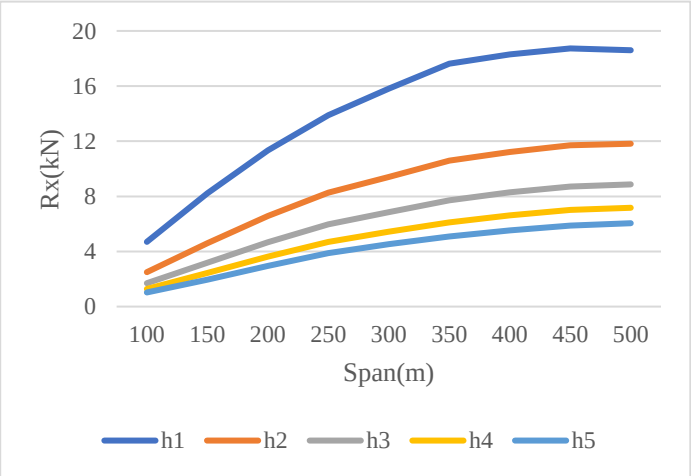

d_{pmin} = 0.044 m, w_{max} = 40N/m, S_{max} = 4%

R_{x7}

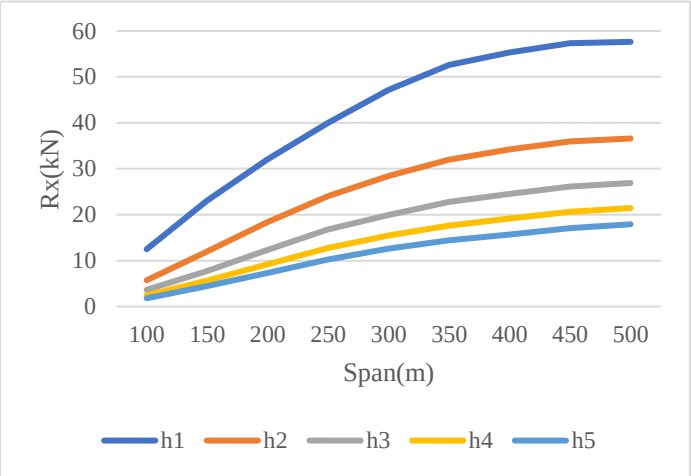

d_{pmax} = 0.08 m, w_{max} = 40N/m, S_{max} = 4%

R_{x8}

3.10 Reference

Aboshosha, H. & A. El Damatty (2014) Effective technique to analyze transmission line conductors under high intensity winds. *Wind and Structures,* 18**,** 235-252.

ASCE. 2020. Guidelines for Electrical Transmission Line Structural Loading. American Society of Civil Engineers Reston, VA.

Dempsey, D. & H. White (1996) Winds wreak havoc on lines. *Transmission and Distribution World,* 48**,** 32-37.

Ekisheva, S., R. Rieder, J. Norris, M. Lauby & I. Dobson (2021) Impact of Extreme Weather on North American Transmission System Outages.

El Damatty, A. & A. Hamada (2016) F2 tornado velocity profiles critical for transmission line structures. *Engineering Structures,* 106**,** 436-449.

El Damatty, A., M. Hamada & A. Hamada. 2015. Simplified F2-Tornado load cases for transmission line structures. In *14th International Conference on Wind Engineering, Porto Alegre, Brazil*.

El Damatty, A. A., N. Ezami & A. Hamada. 2018. Case study for behaviour of transmission line structures under full-scale flow field of Stockton, Kansas, 2005 tornado. In *Electrical Transmission and Substation Structures 2018: Dedicated to Strengthening our Critical Infrastructure*, 257-268. American Society of Civil Engineers Reston, VA.

Fujita, T. T. (1981) Tornadoes and downbursts in the context of generalized planetary scales. *Journal of the Atmospheric Sciences,* 38**,** 1511-1534.

Grasso, L. D. & W. R. Cotton (1995) Numerical simulation of a tornado vortex. *Journal of Atmospheric Sciences,* 52**,** 1192-1203.

Hamada, A. & A. El Damatty (2015) Failure analysis of guyed transmission lines during F2 tornado event. *Engineering Structures,* 85**,** 11-25.

Hamada, A., A. El Damatty, H. Hangan & A. Shehata (2010) Finite element modelling of transmission line structures under tornado wind loading. *Wind and Structures, An International Journal,* 13**,** 451.

Hangan, H. & J. Kim (2008) Swirl ratio effects on tornado vortices in relation to the Fujita scale. *Wind and Structures An International Journal,* 11**,** 291-302.

Hong, H. P., Q. Huang, W. J. Jiang, Q. Tang & P. Jarrett (2021) Tornado wind hazard mapping and equivalent tornado design wind profile for Canada. *Structural Safety,* 91**,** 102078.

Ishac, M. F. & H. B. White. 1994. Effect of tornado loads on transmission lines. In *Proceedings of IEEE/PES Transmission and Distribution Conference*, 521-527. IEEE.

Leslie, L. & R. Smith. 1982. Numerical studies of tornado structure and genesis. In *Intense Atmospheric Vortices*, 205-213. Springer.

Madugula, M. K. 2001. *Dynamic response of lattice towers and guyed masts*. ASCE Publications.

McDonald, J. R., K. C. Mehta, D. A. Smith & J. A. Womble. 2010. The enhanced Fujita scale: Development and implementation. In *Forensic Engineering 2009: Pathology of the Built Environment*, 719-728.

Narancio, G., D. Romanic, J. R. Chowdury & H. Hangan. 2020. Tornado Hazard and Exposure Model for Canadian Communities.

Panneer Selvam, R. & P. C. Millett (2005) Large eddy simulation of the tornado-structure interaction to determine structural loadings. *Wind and Structures,* 8**,** 49-60.

Rotunno, R. (1977) Numerical simulation of a laboratory vortex. *Journal of Atmospheric Sciences,* 34**,** 1942-1956.

Sarkar, P., F. Haan, W. Gallus Jr, K. Le & J. Wurman. 2005. Velocity measurements in a laboratory tornado simulator and their comparison with numerical and full-scale data. In *Proceedings of the 37th Joint Meeting Panel on Wind and Seismic Effects, Tsukuba, Japan, May*.

Savory, E., G. A. Parke, M. Zeinoddini, N. Toy & P. Disney (2001) Modelling of tornado and microburst-induced wind loading and failure of a lattice transmission tower. *Engineering structures,* 23**,** 365-375.

Selvam, R. P. & P. C. Millett (2003) Computer modeling of tornado forces on buildings. *Wind and Structures,* 6**,** 209-220.

Walko, R. 1990. Generation of tornado-like vortices in nonaxisymmetric environments. In *Proceedings of the AMS 16 th Conference On Severe Local Storms*, 583-587.

Wilson, T. 1977. Tornado structure interaction: a numerical simulation. California Univ., Livermore (USA). Lawrence Livermore Lab.

Wilson, T. & R. Rotunno (1986) Numerical simulation of a laminar end-wall vortex and boundary layer. *The Physics of fluids,* 29**,** 3993-4005.

Xia, J. 2001. *Large-eddy simulation of a three-dimensional compressible tornado vortex*. West Virginia University.

Zhang, Y. (2006) Status quo of wind hazard prevention for transmission lines and countermeasures. *East China Electric Power,* 34**,** 28-31.

Chapter 4

4 Conclusions and Recommendations for Future Work

4.1 Summary

The primary concerns of this Thesis are to estimate the conductor's response under tornado loading, and to develop a simple interpolation procedure that can quickly calculate the critical conductor longitudinal reaction under F2 tornado wind loads. To estimate the critical reaction, the following studies are performed:

In Chapter 2, three tornado wind fields simulated and validated previously are considered. All of the wind fields are scaled-up into F2 category. Validation is provided for the semi-analytical technique used to calculate the force transmitted from the conductors to the tower of interest under tornado wind load in this Chapter. Multiple analyses are conducted to validate the number of spans of the considered conductor system. Then, two parametric studies considering eight conductors and three tornadoes is conducted to evaluate the parameters leading to peak longitudinal and transverse reactions transferred from the conductors to the tower of interest: Total Parametric Study, which considers a large range of tornado distance, and the Peak Profile Study, which focuses on the particular value of tornado distance corresponding to the peak vertical profiles on the tower.

In Chapter 3, the parameters leading to peak longitudinal conductor forces estimated in Chapter 2 are employed. A parametric study is first conducted to assess the variation of longitudinal force with different conductor geometric parameters. Based on the results of this parametric study, a set of charts are developed for quick estimation of longitudinal force transmitted from conductors to the tower of interest.

4.2 Conclusions

The conclusions of the studies conducted in Chapter 2 can be summarized as follows:

a) Six spans of conductors is sufficient for an accurate estimation of conductor's longitudinal force Rx

b) The results of Total Parametric Study show that for longitudinal reactions, the critical tornado design parameters are: the Design Tornado and STV1 tornado, with conductor height H = 50 m, tornado distance R equals to the span length, and tornado angle θ = 90°. For the transverse reactions, the critical tornado design parameters are: the STV1 tornado, with H = 50 m, R = 300 m, and θ = 90°.
c) The results of Peak Profile Study show that for longitudinal reactions, the critical tornado design parameters are: the Design Tornado, with H = 30 m and 35 m, R = 125 m and θ = 15° and 30°. For the transverse reactions, the critical tornado design parameters are: the STV1 tornado, with H = 45 m, R = 250 m, and θ = 90°.

The conclusions of the studies conducted in Chapter 3 can be summarized as follows:

a) Rx decreases nonlinearly as the conductor weight increases. If dividing the range of the conductor weight into two regions, Rx changes linearly within each region.
b) Rx increases nonlinearly as the conductor projected area increases. If dividing the range of the conductor projected area into two regions, Rx changes linearly within each region.
c) Rx changes linearly with the sag ratio.
d) Rx changes nonlinearly with insulator length.
e) The Young's Modulus has no obvious effect on Rx.
f) A set of charts are developed which can be used to estimate peak conductor longitudinal forces by adopting a multi-variable line regression. This simple approach is validated and proved to be accurate.

4.3 Recommendations for future work

Based on the outcome of the current Thesis, the following directions are suggested for further exploration:

-Expand the study by focusing on the dynamic effect of conductors under tornado wind load.

-Expand the study by verifying the full-correlation assumption when scaling up the tornado wind field into F2 category.

-Validate the simplified procedure by conducting WindEEE experiments and comparing the experimental results with the numerical results.

-Include the turbulence component of the tornado into the conductor analysis.

Curriculum Vitae

Name:	Dingyu Yao
Post-secondary Education and Degrees:	South China University of Technology Guangzhou, Guangdong, China 2015-2019 B.Eng The University of Western Ontario London, Ontario, Canada 2020-2021 M.Sc
Related Work Experience	Teaching Assistant The University of Western Ontario 2020-2021

Publications:

Yao, Dingyu, El Damatty, A.A, 2020. Critical longitudinal forces in conductors under tornadoes, in: Proceedings of the 2020 World Congress on Advances in Civil, Environmental, & Materials Research (ACEM20).Korean